University of Alberta

The Involvement of Filamentous Actin in Nuclear Processes

by

Carmen Rosa Tomkinson 

A thesis submitted to the Faculty of Graduate Studies and Research in partial fulfillment of the

requirements for the degree of Master of Science

in

Medical Sciences - Oncology

Edmonton, Alberta

Fall 2004

Your file Votre référence
ISBN: 0-612-95869-8
Our file Notre référence
ISBN: 0-612-95869-8

TABLE OF CONTENTS

LIST OF TABLES

Table **Page**

LIST OF FIGURES

Figure **Page**

Chapter 1: Introduction

Section 1.1. Overview of Actin

Actin was first discovered in 1941-1942 as part of the acto-myosin complex responsible for the contractile force in rabbit skeletal muscle [1]. It is an abundant protein with multiple functions in living cells. One of the earliest recognized functions of actin was its assembly into polymers to form the thin filament of sarcomeres. It also has a well-established structural role in the cytoskeleton, and stress fibers. This ubiquitous protein has numerous structural and functional roles from providing mechanical strength to mediating signal transduction pathways.

The genes and functions of actin have been highly conserved throughout evolution [2]. Although some eukaryotes have only a single actin gene many multicellular organisms have several actin genes that code for different isoforms. Mammals have at least six types of actin that fall into three different categories depending on their isoelectric points [3]. Although the α-actin isoform of vertebrates muscles cells varies at only a few positions from the β- and γ-actin isoforms present in non-muscle cells these variations result in different functions [4]. The different isoforms are also expressed in a tissue specific manner with the relative proportions being dependent on cell type [5,6].

Actin typically carries out its functions while in the filamentous state. Thus, controlling the polymerization of globular actin (G-actin) into filamentous actin (F-actin) can in turn modulate activities in the cell. The polymerization of actin is

achieved in two stages, nucleation and elongation. First, nucleation involves weak binding between two monomers followed by a third monomer binding to stabilize the structure [7]. The kinetic barrier to nucleation results in the rate-limiting step causing a lag phase, which is followed by rapid polymerization (Figure 1-1). The number of actin monomers that are added per second during polymerization is proportional to the concentration of free subunits [8]. However, shortly after polymerization the ATP molecule bound within actin is hydrolyzed to ADP creating a conformational change to the actin subunit that promotes disassembly. Thus the critical concentration, below which polymerization does not occur, is determined by the number of subunits coming off the polymer divided by the number of subunits assembling [8]. When there is equilibrium between the addition and the loss of subunits to the polymer a steady-state stage is reached called the equilibrium phase.

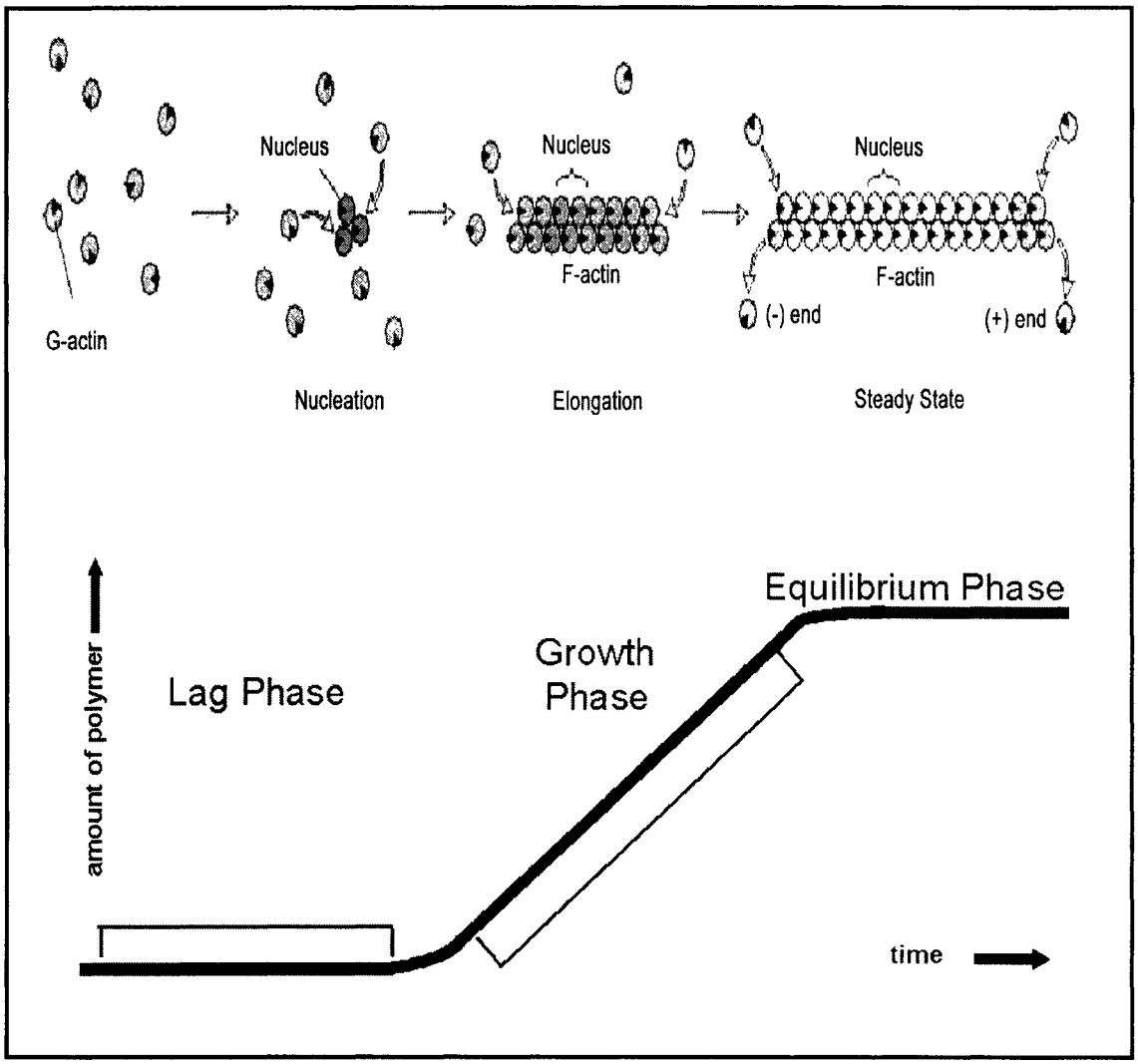

Figure 1-1. Actin polymerization depicted in three stages. The initial nucleation phase is achieved through binding of actin monomers into a stable actin nucleus. Monomers are then rapidly added unto the nuclei during the elongation phase and finally the equilibrium phase is achieved when the ends of actin are at a steady state. Adapted from Lodish *et al.* 2000 [9].

The assembly of subunits onto a polymer does not occur at the same rates for both ends of the filament. The barbed end (plus-end) is found to have a critical concentration requirement that is 12-15 fold lower than that of the pointed end (minus-end) and thus has a much faster rate of assembly [10]. This concept results in an interesting activity called treadmilling where the plus-end has a net assembly of subunits whereas the minus-end has a proportional net loss of subunits so that the overall length of the filament does not change although subunits cycle through the filament (Figure 1-2) [11]. The difference in rates of polymerization is due to structural differences between the plus and minus ends caused by the conformational changes in response to ATP hydrolysis.

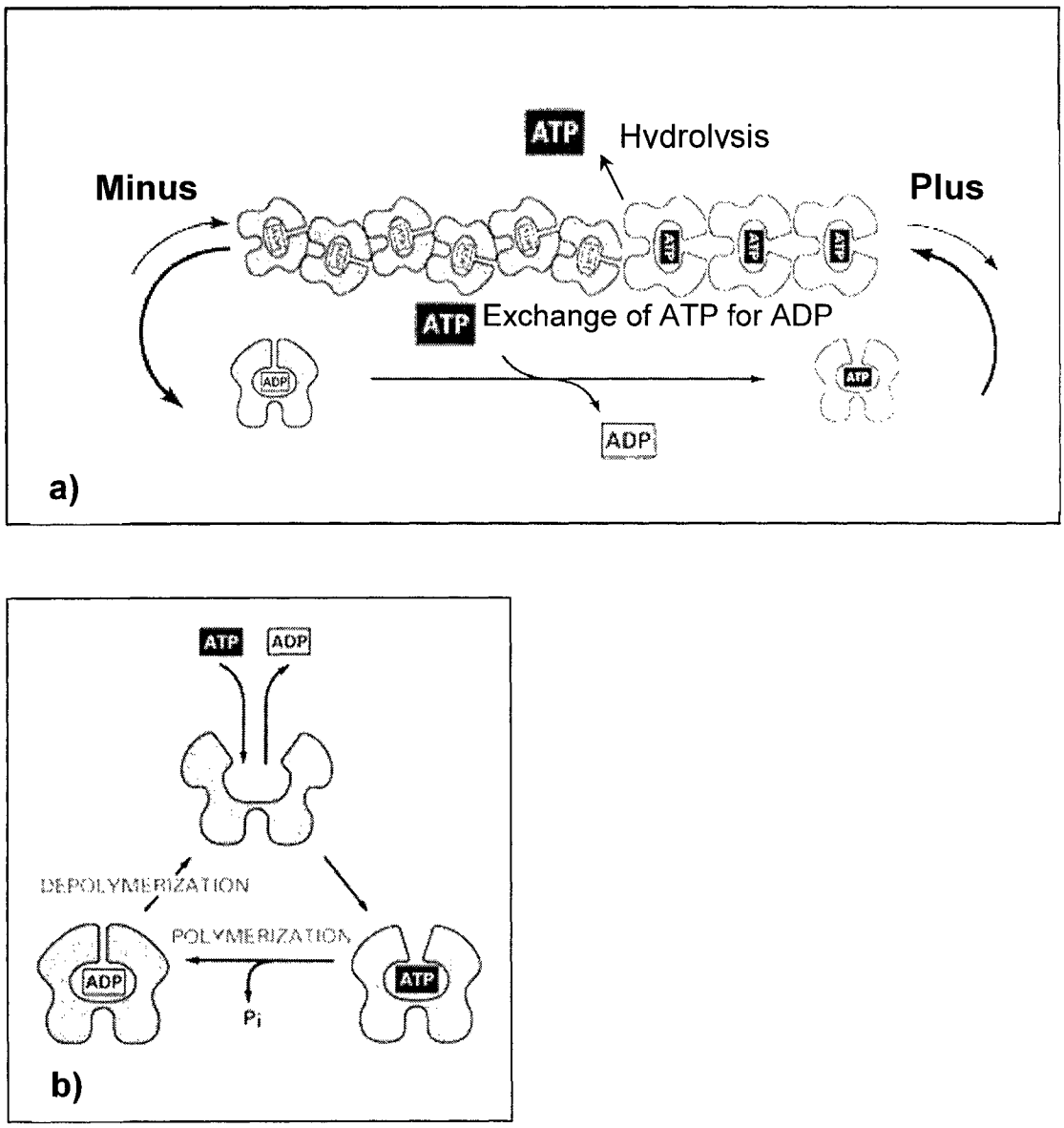

Figure 1-2. Actin filaments trap ADP and undergo the process of treadmilling. a) Treadmilling occurs when actin monomers are continually added to the filament plus end and lost from the minus end with no net change in filament length. b) The two domains of actin are hinged around an ATP binding site. When the molecule becomes incorporated into a filament the ATP is hydrolyzed to ADP. For the ADP to be replaced by ATP the hinge has to be opened which happens when the filament depolymerizes. Normally interactions between subunits in the filament prevent the hinge from opening. Adapted for Alberts *et al.* 1994 [7].

Section 1.2. Nuclear Actin

Section 1.2.1. Findings of nuclear filamentous actin

The fact that actin plays numerous cytoplasmic roles begs the question of whether or not actin is in the nucleus and if so, does it have functions in nuclear processes? A number of early studies reported the presence of actin in the cell nucleus of non-muscle cells [12-14]. However, these claims were largely discounted since even minor contamination from the abundant cytoplasmic actin could result in a seemingly significant amount of nuclear actin. The careful hand isolation of large nuclei from *Xenopus* oocytes, in early prophase and enlarged due to protein accumulation, helped to dispel this controversy [15]. Puncturing the plasma membrane and squeezing the cell with forceps expelled the nucleus and the nuclear envelope could be stripped away using tweezers [15]. The identification of actin in the nuclei was achieved using several criteria. First, SDS-polyacrylamide gel electrophoresis revealed both the total nuclei and the nuclear gel fractions to contain a 43,000-dalton polypeptide that co-migrates with actin [15]. The gel was fixed and assayed for cross-reactivity with antiserum against skeletal muscle actin and showed the only labeled band co-migrated with actin in the gel preparations [15]. Furthermore, DNase I, which binds specifically to actin, was found to interact with the 43,000-dalton polypeptide as found by the use of a DNase I-agarose affinity column [15]. Although the culmination of these findings identify actin as a component of the nucleus, the presence of nuclear actin remained controversial until only recently.

The idea that *Xenopus* oocytes may be an exceptional case with respect to nuclear actin was a common criticism. This skepticism was galvanized by the failure of some to detect binding of fluorescently labeled phalloidin to nuclear F-actin [16]. However, both of these doubts can be easily refuted. First, there have been numerous subsequent studies, using a variety of techniques and cell types, which have identified actin in the nucleus [17-24]. The consistency of these findings despite different cell types has dispelled doubt of *Xenopus* oocytes as a special case. Now, the controversy lies in the questions of where in the nucleus actin is distributed and the dynamics of its form as monomers or polymeric actin. The lack of phalloidin staining may reflect either an inaccessibility of the binding site or the predominance of monomeric actin or short oligomers as opposed to the filaments that phalloidin binds [16]. If the amount of nuclear actin is below the critical concentration for polymerization then filaments would not initiate. Some studies have detected phalloidin binding to nuclear actin. In 1988, the incubation of the myxamoebae and macroplasmodia of the slime mold *Physarum polycephalum* in a phalloidin-gold complex showed the nucleoplasm to be more intensely labeled than the cytoplasm [25]. The fact that different experimental methods produce different results has clouded the reality of what form nuclear actin is normally found in.

Actin contains two leucine-rich sequences that can drive nuclear export. Nuclear actin may exist in a monomeric state because export from the nucleus could maintain actin concentrations lower than that necessary to support polymerization [26]. To investigate whether or not the distribution of actin is regulated by the nuclear export sequences a specific inhibitor of nuclear export, leptomycin B is used. Prior to

any drug treatment, staining with anti-actin antibodies showed actin to be predominantly cytoplasmic, however after leptomycin B treatments actin localizes to the nucleus where it forms lattice-like structures [26]. Although these findings indicate a potential mechanism for maintaining a reduced concentration of nuclear actin, estimates of nuclear actin concentration indicate that there are significant quantities of nuclear actin for the formation of filaments. Initial studies by Clark and Merriam found approximately 75% of actin to be diffusible suggesting the other 25% is either in larger filaments or associated with other structures [15].

Currently, a valuable tool for investigating the dynamics and distribution of nuclear actin is fluorescence recovery after photobleaching (FRAP) and green fluorescent protein (GFP)-fusion proteins. McDonald *et al.* utilized HeLa cells stably expressing GFP-beta-actin to monitor the recovery of actin back into areas of the nucleus that had been photobleached with an argon laser [27]. The data on rates of recovery of GFP-actin can be applied to mathematical models to determine the dynamics of nuclear actin molecules. However, first it is important to know that the behavior of GFP-actin approximates that of endogenous actin. Through the use of time lapse microscopy it was observed that GFP-actin incorporates into F-actin structures and assembles and disassembles in the expected way [27]. Furthermore, the distribution of nuclear GFP-actin and microinjected Rhodamine-actin are the same, with homogenous distribution through out the nucleoplasm and a lower concentration in the nucleoli [27]. The relative amounts of polymeric and monomeric actin can be determined by photobleaching and monitoring the recovery of GFP-actin back into the bleached areas. In the cytoplasm the fast recovering population, representing

monomeric actin, accounts for 70% of the total GFP-actin pool whereas in the nucleus 80% of the GFP-actin is in its monomeric state [27]. To help corroborate that the 20% of slow recovering nuclear GFP-actin may be F-actin, cells were treated with the drug latrunculin, which disrupts actin filaments by sequestering actin monomers. Results from FRAP experiments show that the slow recovery phase is eliminated due to the latrunculin treatments [27]. This result was confirmed by using a microinjected FITC-labeled anti-beta actin antibody that has a recovery profile that is superimposable upon the GFP-beta actin recovery profile [27].

In the cytoplasm the turnover of actin molecules in filaments determines the recovery properties rather than the diffusion of the large filaments themselves. Interestingly the recovery profile of nuclear actin parallels the recovery profile of cytoplasmic actin suggesting that turnover is also the factor responsible for the slow recovery phase of nuclear actin. Mathematical models can be used to help test the molecular basis for the flux of molecules in FRAP experiments. The mathematical simulations can define the molecular weight required to generate a diffusion-based mobility of the rate observed. Since the mass predicted for the recovery curves requires such high molecular weight complexes it is unlikely that the recovery of actin is described by the diffusion of a massive complex. Instead it is more probable that actin exists in a network with the recovery kinetics determined by the dynamic exchange of molecules into and out of an F-actin containing structure.

Section 1.2.2. Controlling Actin Dynamics in the Nucleus

The presence of many actin-binding proteins, as well as their chief regulators calcium and phosphatidylinositol (4,5)-bisphosphate (PtdIns(4,5) P_2), in the nucleus suggests that the dynamics and polymerization of nuclear actin may be controlled. There are multiple types of nuclear actin-binding proteins including, those whose small size allows diffusion into the nucleus, those with nuclear localization sequences, those which relocate in response to stress or heat shock, and those that bind specifically to actin but have unknown functions.

Two well-known actin-binding proteins found in the nucleus are thymosin, a sequestering protein, and profilin, a sequestering and nucleotide exchange protein [28]. However, the fact that they are small enough to diffuse into the nucleus puts the physiological significance of their nuclear activity into question. There are other proteins that contain nuclear localization sequences to the nucleus and have been shown to have actin-binding activities *in vitro.* For example, the tyrosine kinase c-Abl, is involved in the cellular response to DNA damage [29]. Analyses with deletion mutants have identified the extreme COOH-terminus of c-Abl to be responsible for interactions with F-actin. Furthermore, the COOH-terminus of c-Abl contains a proline-rich region that mediates binding and sequestering of G-actin, and the F- and G-actin binding domains cooperate to bundle F-actin filaments *in vivo* [29].

Another interesting class of nuclear actin-binding proteins are those that localize to the nucleus in a regulated manner and have a well-characterized association with actin. For example, myopodin is a novel actin binding protein that

accumulates in the nucleus in response to stress conditions, which also cause the localization of actin to the nucleus [30,31]. In the cytoplasm myopodin binds to stress fibers before incorporating into Z-discs, which are sites of the cross-linked actin filaments in sarcromeres. Therefore, it is proposed that myopodin is a structural protein that contributes to signaling pathways between the Z-disc and the nucleus [30]. Another example is CapG, a gelsolin-like capping protein with at least partial localization to the nucleus [32]. The fact that CapG is phosphorylated *in vivo* and when isolated from the nucleus is found to be predominantly phosphorylated suggests that phosphorylation is the event required for nuclear entry [33]. Cofilin, an actin-severing protein also translocates to the nucleus in a phosphorylation dependent manner, however unlike CapG, the localization event is a result of dephosphorylation of serine 3 [34]. Interestingly, the phosphorylation of serine not only is counter to nuclear entry but also prevents cofilin from severing actin filaments [35]. This dephosphorylation and translocation to the nucleus occurs upon heat shock, treatment with DMSO, and costimulation of T cells [36-38]. Interestingly, conditions of heat shock and DMSO also induce reorganization of actin from stress fibers to intranuclear actin rods, which coincides with the synthesis of several heat shock proteins [31].

In 1999, a functional link was established for cofilin in the nucleus by studies of serum response factor (SRF)-dependent gene transcription, which determined a role for the serine/threonine kinase LIMK-1, its substrate cofilin, and actin dynamics in SRF reporter activation [39]. The serine/threonine kinase, LIMK-1, phosphorylates cofilin at serine 3 and prevents its interaction with actin therefore promoting the formation of F-actin aggregates. It was shown that LIM kinases specifically activate

SRF-linked signal pathways. Microinjection experiments were used to determine whether effects on F-actin mediated this activation. When NIH3T3 cells were microinjected with LIMK and cofilin expression plasmids, as well as an SRF-controlled reporter gene, it was found that LIMK and wild-type cofilin activated the reporter gene [39]. However, when serine 3 of cofilin is mutated, the formation of actin aggregates by LIMK-1 is blocked, and the activation of the SRF-reporter gene is inhibited [39]. This result suggests that the ability of LIMK-1 to activate SRF is dependent on its control of actin treadmilling. In support of this suggestion is the finding that latrunculin B treatments, which decrease the amount of F-actin, also inhibit activation of the SRF-controlled reporter gene and drugs that promote F-actin accumulation such as jasplakinolide also activate SRF [39]. Further studies using actin mutants show that expression of mutants favoring F-actin formation strongly activate SRF whereas actins that cannot polymerize are effective inhibitors of SRF [40]. It seems SRF activity is mediated by a decrease in G-actin rather than an increase in F-actin since drugs that bind actin without promoting F-actin formation result in an increase in SRF activity [40]. Taken together these results present evidence for a role of monomeric actin in the signaling of SRF.

Another class of nuclear actin-binding proteins are those which have well-established functions in the cytoplasm but whose nuclear roles are unclear. One such protein is the structural protein 4.1 that links spectrin-actin complexes to plasma membrane-associated proteins in the human red cell membrane skeleton [41]. In mammalian cell nuclei, 4.1 and actin colocalize as detected by immunofluorescence microscopy [42]. More detailed information comes through the use of immuno-electron

microscopy that shows localization of nuclear actin and protein 4.1 with nuclear filaments [42]. Furthermore, during nuclear assembly actin forms a network-like pattern that colocalizes extensively with protein 4.1. Although the extensive actin network has sites independent of 4.1, the signal that does overlap is most coincident in early stages of assembly and continues to colocalize to some extent in later stages [42]. When either actin or 4.1 are inhibited neither are incorporated into nuclei and nuclear assembly is blocked [42]. Although the details of 4.1 interactions with nuclear actin are unknown the evidence does suggest that it may be critical to nuclear assembly. As well, protein 4.1 interactions with actin may have a role in RNA splicing as shown by some areas of 4.1-actin that colocalize with splicing centers [42]. Previously, protein 4.1 has been shown to co-immunoprecipitate with multiple splicing factors and 4.1 depletion inhibits RNA splicing *in vitro* [41]. Nevertheless, the very presence of protein 4.1 and numerous other nuclear actin-binding proteins suggests that not only may actin be involved in nuclear processes but its dynamics could be controlled.

Section 1.3. Nuclear Architecture

Section 1.3.1. Findings of a 'nuclear matrix'

The nucleus was once viewed as an unorganized organelle despite the complexity of nuclear processes such as replication, repair, and transcription, which suggest the necessity for an organized architecture. In 1974, Berezney and Coffey

coined the term 'nuclear matrix' to refer to the structure that remains after 2 M NaCl extraction strips histones from DNA and DNase digestion detaches most of the DNA [43]. However, skepticism stemmed from the notion that extraction procedures induce precipitation of soluble proteins and alters protein interactions. These criticisms stimulated many variations of this protocol, including a notable experiment by Capco, Wan and Penman, which used a lower salt concentration to elute the digested chromatin and then visualized the nuclear remnants by whole mount microscopy [44]. Visualization by electron microscopy revealed a three-dimensional anastomosing network of filaments ranging in diameter from 3-22 nm [44]. Although this was a clearer view in comparison to earlier experiments using thin sections embedded in plastic, there was still skepticism over the high ionic strength buffers used. This prompted others to use more physiological strength buffers that surprisingly revealed the same anastomosing internal matrix. For example, in 1985 Jackson and Cook used an elegant method of encapsulating cells in agarose followed by a detergent lysis in the presence of an isotonic salt buffer [45]. The large pore size of the agarose allowed for diffusion of RNA and many cytoplasmic proteins out of the nucleus. The remaining encapsulated chromatin was still accessible to digestion and removal revealing a nuclear matrix that closely resembled that prepared by higher salt extraction procedures [45].

In addition to evidence from microscopy there are still other reasons to believe that nuclear structure exists and is capable of organizing the nucleus. Some of the most compelling evidence for a spatially organized nucleus comes from the finding that chromosomes occupy their own discrete domains [46]. The dynamics of

how chromatin territories are maintained has been somewhat controversial. In 1997, Abney *et al.* found chromatin to be immobile over distance scales larger than 0.4μm claiming the motion of chromatin to be impeded by a highly concentrated nuclear content or by direct attachment of the chromatin to a nuclear matrix [47]. However, in the same year, Marshall *et al.* published a paper stating that the nucleus is not a static structure with immobile chromosomes arguing that fundamental nuclear processes require chromosomal movement [48]. By quantitatively tracking the movement in real time of GFP labeled yeast chromosomes, Marshall *et al.* concluded that chromosomes do undergo motion albeit confined to very small nuclear regions [48]. The proposed explanation is that chromosomes have successive attachment points that partition the individual chromosome into further domains. Thus, the attachment of domains of chromosomes to an immobile structure would result in "constrained diffusion" [48]. Investigation of the many other compositionally discrete domains, including splicing factor compartments, the Cajal body, the promyelocytic leukemia (PML) body, and RNA processing machinery domains, has provided additional insight into how compartments are maintained [49-53]. In particular, investigating the mobility of the splicing factor ASF has been informative. Using ASF-GFP fusion protein and photobleaching microscopy it was revealed that ASF-GFP has a mobility that is 100 times slower than free diffusion [54,55]. A likely explanation for this reduction in mobility is that the splicing factors have frequent transitory interactions with an underlying structure. This nuclear structure may also act as a physical barrier resulting in "obstructed diffusion" [56]. The relatively wide range of mobility of small 40nm fluorescent beads in comparison to PML bodies suggests considerable variation

in the density of the nucleoplasm [56]. These small beads are able to enter areas of high density where they become immobilized. The limited ability for movement of these small beads suggests a much more structured nucleoplasm with a higher abundance of physical barriers than previously expected.

Section 1.3.2. Actin as a component of nuclear architecture

In simplest terms the nuclear matrix can be defined as the non-chromatin structures of the nucleus. The principal feature of these non-chromatin structures was identified in the early 1960's to be the fibrogranular ribonucleoprotein (RNP) network [57]. However, quantitative analysis of elemental phosphorus and nitrogen using electron spectroscopic imaging (ESI) demonstrates that the majority of the structure within the interchromatin regions is not ribonucleoprotein [58]. This analysis uses a conventional electron microscopy with analytical imaging spectometer. ESI is able to elucidate the mass and nucleic acid content in nucleoprotein complexes by imaging with electrons that have a specific energy loss due to interactions with electron shells of the atoms within the specimens of phosphorus and nitrogen atoms [58]. A net nitrogen image will reflect the density of protein, and when the interchromatin space is observed in this image it appears filled, indicating an abundance of protein-rich, nucleic acid-depleted structure [58]. The protein composition of this structure is unknown however one obvious candidate is actin. Numerous studies have found a nuclear matrix protein that cofocuses with actin in two-dimensional gel electrophoresis [22,44,59,60]. Even more compelling are *in vitro*

findings that nuclear actin is required for nuclear assembly. An assay to image nuclear actin without fixation or expression of fusion proteins was created by covalently labeling actin with rhodamine, adding it to *Xenopus* egg extracts and, initiating nuclear assembly by demembranated *Xenopus* sperm [42]. Fluorescence microscopy images show actin as being first detected when chromatin and nuclear pores begin to assemble. As the nuclear assembly progresses detection of actin is more pronounced and the emergence of a lattice structure occurs. The assembly of this discrete network happens during lamina and pore formation but before DNA synthesis [42]. To confirm that filamentous actin is in fact necessary for this assembly the inhibitor latrunculin A is used. The nuclei that form in response to drug treatment and therefore actin depletion are small, distorted, and incapable of DNA synthesis [42]. These findings suggest that F-actin is a necessary component in maintaining nuclear architecture and therefore the potential importance of actin in nuclear processes is vast.

Section 1.4. Implications of Nuclear Architecture

Section 1.4.1. Functional nuclear compartmentalization

Nuclear processes such as replication, transcription, RNA processing, and DNA repair, are complex and a highly organized nucleus can ensure the regulation and coordination of these systems. One type of functional organization is the arrangement of chromosomes into discrete domains dictated in part by functional

activity. Under certain conditions, fluorescence hybridization has revealed that transcriptionally active sequences can be visualized as highly condensed individual spots whereas transcriptionally inactive sequences are shown as long loops [61]. This is consistent with the loop domain organization of chromatin packing that views transcriptionally active sequences as being in between matrix attachment regions (MARs) and therefore immobilized on the nuclear matrix whereas the nontranscribed chromatin is in condensed higher-order supercoiled loops [62]. Support for this comes from findings that chromatin with highly acetylated histones, a common marker for transcriptionally active DNA, is found enriched in nuclear matrix fractions [63]. The condensed structure of the transcriptionally inactive sequences makes them hidden to transcription machinery and transcription factors while on the other hand; the transcriptionally active genes are DNase I-sensitive and presumed to be easily accessible [64]. The most sensitive regions are functionally important, often promoters, enhancers, and sites of nuclear matrix attachments, and are found to be especially sensitive to nuclease cleavage due to chromatin structural changes necessary for transcription [65]. Additional evidence for the importance of chromatin domains on transcriptional activity comes from studies on position effect variegation (PEV) that show the expression of a gene depends on its chromosomal position [66]. The chromosomal rearrangement of a normally active gene to a position adjacent to a transcriptionally inactive heterochromatic region leads to the inactivation of the gene [67]. PEV was first seen in *Drosophila* when inversion of the X chromosome moving the *white* gene closer to heterochromatin results in increased repression of the *white* gene. The degree of repression depends on the proximity of the gene to the

heterochromatin with the highest repression being when the gene is closest to the heterochromatin [67]. Many of the genes that are able to suppress transcription by positional effects have been characterized and interestingly they are able to alter the organization of chromatin [68].

There are many other organized subcompartments in addition to those of chromosomes territories and, importantly, there is a distinct spatial relationship between these compartments. Transcriptionally active genes tend to be found at the periphery of chromosome territories and fluorescence *in situ* hybridization shows nascent transcripts and splicing machinery to be excluded from the interior of chromatin territories [69,70]. Furthermore, there is evidence that areas of intense transcription often occur at the border of intranuclear structures termed interchromatin granule clusters (IGC) [71]. IGC accrue splicing machinery, pre-mRNA and polyadenylated mRNA suggesting they represent sites of pre-mRNA processing and mature mRNA accumulation [72-74]. Fluorescence antibody staining has revealed condensed heterochromatin to be enriched on the nuclear edge and absent from IGCs as recognized by antibodies to the splicing factor SC-35 [75]. The distribution of transcriptionally competent euchromatin can be determined using antibodies to acetylated histones. Through the use of these antibodies, euchromatin is shown to be absent from the nuclear periphery, where heterochromatin likely acts in nuclear attachment, and instead is often localized at the borders of IGCs [75]. $TAF_{II}250$, which is a component of RNA polymerase II complexes, also colocalizes with the acetylated chromatin at the periphery of IGCs [75]. Although some transcriptionally active areas are located at IGCs, this clearly represents only a subset of transcription. Still,

investigating transcription in relation to IGCs is a useful example of coordination between compartments. By concentrating components required for transcription and RNA processing this complex system can exert a high level of regulation and fidelity.

Section 1.4.2. A paradigm: nucleolar transcription factories

The best paradigm for nuclear organization may be the creation of rRNA by polymerase I in nucleolar transcription factories. The well-characterized activities of ribosomal gene transcription, rRNA processing, and the pre-ribosomal particle assembly are a useful model for functional compartmentalization [76]. When viewed by electron microscope, nucleoli contain several light zones called "fibrillar centers" surrounded and interconnected by crescent-shaped "dense fibrillar components" which are, in turn, embedded in "granular components" [77]. Incubation with either Br-uridine or Br-UTP to immunolabel Br-RNA with gold particles revealed the label to be concentrated at the border between fibrillar centers, which were unlabeled except at their periphery, and dense fibrillar components [77]. Multiple studies using antibodies and hybridization probes show the fibrillar centers to be rich in ribosomal RNA genes, RNA polymerase I, the class I gene transcription factor UBF, and toposiomerases [78-82]. It is inferred that the fibrillar centers are storage sites for transcriptional machinery with active transcription occurring at the surface and nascent rRNA transcripts being extruded into the dense fibrillar components. Hybridization probes to unprocessed transcripts and the associated processing machinery localize to the dense fibrillar components [83-85]. Upon termination of the

nascent rRNA it moves to the granular component to complete maturation. Partially processed transcripts, intermediates in ribosome assembly, and mature 28S and 18S rRNA are all found in the granular region. Taken together the fibrillar center coupled with its dense fibrillar component can constitute one nucleolar transcription factory that releases a transcript to the granular component. Depending on the rate of rRNA synthesis, these factories differ widely in diameter and the number of transcription units and associated polymerases. Normally each factory is associated with one, or a few, active ribosomal cistrons and the number of factories is reduced or increased depending on levels of transcription. For example, conditions of serum starvation result in ~234 factories in a normally growing fibroblast aggregating into ~156 factories [86]. On the other hand, when a lymphocyte in the peripheral blood is stimulated to divide the ~9 factories divide and rise to ~80 [87]. In other words, when transcription is increased the transcription factories have a higher cumulative surface area in turn increasing the number and accessibility of polymerases to promoters. In very active cells, factories can split so that each ribosomal transcriptional unit becomes associated with one small factory [88]. In the case where transcription is decreased the transcription factories combine and store the polymerases that are not needed.

There is evidence that nucleolar architecture is maintained by structural support that is provided by a nucleoskeleton. When the granular component and the dense fibrillar component are dispersed by a hypotonic treatment and the unattached DNA is digested and electoeluted under physiological conditions the fibrillar centers remained fixed to a nucleoskeleton [77]. One explanation is that the template is

attached to the underlying substructure through active polymerases. The relationship between a variety of loci of the ribosomal gene repeat and the nucleoskeleton were examined further by hybridization with rDNA probes for the transcription unit or for nontranscribed intergenic spacer [89]. The results showed strong signal with probes for the transcription unit but not with the probes for the intergenic spacer indicating that only the transcription unit is strongly attached to the substructure, likely through RNA polymerase complexes rather than through sequence-specific attachment sites [89]. In other words, rDNA is associated with a physical skeleton through fixed transcription sites that pull the DNA through the RNA polymerase I multiprotein complex. The nascent transcript will extrude from this fibrillar center, which is embedded in the nucleoskeleton, and extend into the dense fibrillar component. Then it will move into the granular component to complete maturation and in the end be transported to the cytoplasm. Meier *et al.* used immunoelectron microscopy to visualize the nucleoprotein Nopp140 traveling on tracks from the nucleolus to the cytoplasm [90]. They observed curvilinear tracks that extended from the dense fibrillar component through the nucleoplasm to nuclear pores. The compartmentalization of rRNA synthesis, as well as the evidence for structural support provided by an underlying substructure interacting with elements of the fibrillar centers, provides an interesting model for investigating other nuclear processes.

Section 1.4.3. Evidence for control of nuclear processes through associations with the nuclear matrix

The idea that an underlying physical structure guides the spatial distribution of compartments is supported by findings that polymerases and many functional processing components have associations with the nuclear matrix. The idea that polymerases are much less mobile than usually depicted in textbook models is both theoretical and factually based. If the polymerase is mobile and tracks along a helical DNA template then the transcript would become entwined on the template. To solve this problem either an untwining mechanism has to detangle the transcript, which would be entwined 10^5 times for every 10^6 basepairs, or the DNA must rotate through the polymerase [91]. One reason to favor DNA rotating through an immobilized polymerase is based on size discrepancy. It is much easier to imagine DNA moving through a large immobilized structure rather than a massive multiprotein complex tracking around a DNA template [88]. Furthermore, if the polymerase does track on the template then the necessary untwining mechanism must be precise since untwining even once too few or once too many times would still leave the transcript entangled and unable to escape to the cytoplasm [91]. More direct evidence for immobilized polymerases comes from the finding that nascent transcripts and their templates remain bound to a substructure. It would be expected that tracking polymerases and their transcripts would be stripped from their templates, however cells grown in [92]uridine and then lysed in 2M NaCl do not lose their [^{3}H]uridine [93]. Of course criticism stemmed from the possibility that the transcripts may have precipitated in

the hypertonic conditions used; however the same results were found using more physiological buffers and agarose encapsulation [45,94]. Further convincing evidence that RNA polymerases are not free to track comes from visualization. [^{3}H]uridine, Br-uridine, Br-UTP, or biotin-CTP can be incorporated into newly synthesized RNA by polymerase II and then visualized by either autoradiography, as is the case for [^{3}H]uridine, or immunolabeling with antibodies [91,94]. The results show that new transcripts are concentrated into transcription factories and the factories maintain their spatial organization even in the absence of chromatin [94,95]. However, some problems with determining the exact locations of transcription include the fact that transcripts that are still growing can be pushed from the site or origin in a very short amount of time, as well completed transcripts can diffuse away from the site of polymerization [88]. Fortunately, the use of shorter labeling times and instruments for sensitive detection remedy both of these problems. In this way transcripts are found to be concentrated in discrete foci suggesting that active polymerases must also be concentrated perhaps due to attachment to a substructure [88].

Evidence for immobilized DNA polymerases are even more convincing and since many polymerases have general structural homology it is probable that they function in similar ways. Using DNA precursors newly made DNA was found bound to a substructure or a matrix [96]. However, like similar findings with RNA polymerases, these results were not generally accepted since the high salt buffers could result in artifactual associations. Later the use of physiological conditions resulted in the same finding that nascent DNA resists detachment [97]. Other evidence that DNA polymerases are immobilized comes from visualization of the polymerases

concentrated into foci. During S phase, cells can be incubated with bromodeoxyuridine that incorporates into replicating DNA and visualized through the use of fluorescent antibodies to the analog [98]. Instead of a diffuse staining of the antibody, discrete foci are seen. Also these foci change over the extent of S phase with small discrete foci of early S phase becoming fewer and enlarged as the heterochromatin is replicating [99]. Using electron microscopy, these foci are seen as electron-dense, morphologically discrete bodies strung along a nucleoskeleton with newly replicating DNA associated and extruding from them [100]. These foci remain morphologically and functionally intact even when 90% of the chromatin is removed. If agarose encapsulated cells are incubated with biotin-11-dUTP in 'physiological' buffers for a short amount of time (2.5 minutes), the analog is seen associating with the electron-dense bodies however; longer incubations reveal the analog moving into the neighboring chromatin and eventually labeling a large amount of the chromatin within an hour [100]. These findings give direct visual evidence for DNA polymerization factories being fixed to an underlying structure while a replicating templates move through the structures.

Transcription factors as well as components for RNA processing and posttranslational chromatin modification are also localized to the nuclear matrix and may mediate the dynamics of attachment between chromatin and the matrix [101]. In this way the matrix could control gene expression in part by binding certain transcription factors and concentrating them at specific nuclear sites. It has been shown that the matrix is selective about which transcription factors it binds and that this selectivity varies with cell type [102,103]. Furthermore, the transcription factors that

associate with the matrix change throughout development and differentiation. For example, in primitive red blood cells from 5-day old chick embryos, the nuclear matrix binds transcription factors that are key in particular erythrocyte gene expression [104]. However, in embryos that are 11-days and 15-days old the blood cells are more definitive and the nuclear matrix binds fewer of these transcription factors [104]. The specificity of transcription factors binding to the matrix hints at control of gene expression through a physical substructure.

The fact that histone acetyltransferases (HATs) and histone deacetylases (HDACs) associate with the nuclear skeleton suggests an additional possibility for the matrix to exert transcriptional control [63,105-107]. Transcriptionally active chromatin has high levels of histone acetylation and this modification functions in altering nucleosome structure and the level of chromatin compaction, in turn changing the accessibility for interactions with transcription factors [108-115]. Highly acetylated histones are also quickly deacetylated and this rapid turn over occurs primarily with histones of transcriptionally active chromatin [63,116-118]. Since the chromatin fragments that have these rapidly acetylated and deacetylated histones are attached to the nuclear matrix it follows that HATs and HDACs responsible for this modification would also have matrix associations. Indeed a large percentage (~75-80%) of HDAC activity is retained in the nuclear skeleton of chicken immature erythrocytes as well, HDACs have been found as nuclear matrix components in chicken mature erythrocytes, trout liver, trout hepatocellular carcinoma, and chicken liver [63,107]. HATs have also been shown to be associated with the nuclear matrix. After the

majority of DNA is digested and solubilized the residual nuclear matrix contains 60-76% of the HAT activity [105].

When the nuclear matrix is solubilized some of the HDACs and HATs are released, however, the conventional low-salt extraction procedure as originally described by Dignam *et al.* [119] do not solubilize a representative amount of the total nuclear HDAC's and HAT's [120]. In particular, only 25% and 30% of HDAC1 and HDAC3, respectively, are solubilized in lower salt conditions [120]. Denaturing agents can increase solubility but have the drawback of disrupting protein-protein interactions. When the drug, latrunculin B, is used to disrupt F-actin prior to nuclear isolation and extraction the result is an increase in the solubility of many proteins, including HDACs and HATs, which were less soluble in the low –salt extraction procedure [120]. Importantly, drugs that disrupt other cytoskeletal proteins, such as tubulin, which does not form filaments in the nucleus, do not have significant effects on the solubility. Together these findings suggest that HDACs and HATs are localized on a nuclear matrix that may include F-actin [120]. One potential function is that the association of transcriptionally active chromatin with the nuclear matrix-bound HATs and HDACs results in the immobilization of active chromatin regions onto the nuclear matrix [107].

Section 1.4.4. Coordinating processes through nuclear architecture

In addition to transcription many other nuclear processes, such as replication and repair, are mediated by nuclear structure. Perhaps as a means of coordinating and

controlling these activities, nuclear architecture that favors one nuclear process can exert repression on other processes. For example, it has been shown that certain nuclear domains either have high activity of transcription or replication but never both at the same time [121,122]. Wansink *et al.* incubated permeabilized human bladder carcinoma cells with 5-bromouridine 5'-triphosphate (BrUTP) and digoxigenin-11-deoxyuridine 5'-triphosphate (dig-dUTP) to incorporate into nascent RNA and DNA respectively [121]. Sites of transcription and replication were then visualized using two different fluorochromes to stain the double-labeled nuclei and examination was carried out by confocal microscopy [121]. It was found that throughout S-phase, RNA transcription is concentrated outside replication domains. In late S-phase, when the transcriptionally inactive heterochromatin is predominantly replicated, there is obvious separation between transcription and replication domains. The replication pattern in late S-phase, typified by fewer and larger replication domains, allows for easy detection of this clear distinction between transcription and replication domains [121]. However, during early S-phase when most actively transcribed genes are replicated the domains are small and dispersed making it more difficult to distinguish between domains. Using the double-labeling procedure, cells in early S-phase have transcription pattern that appear very similar to the replication patterns, however the domains do not colocalize. Bivariate histograms examining individual voxels confirms this by showing there is indeed little overlap between voxels with high activity of replication and those with high levels of transcription. These findings are further verified by work from Berezney *et al.* using three-dimensional analysis [122]. They found that although network patterns of replication and transcription domains

may appear similar they actually occupy entirely separate areas of the nuclear volume and the small percentage of the domains that appear to overlap are actually in different levels in three-dimensional space instead of overlapping at a specific site [122]. It is proposed that the spatial patterns of higher order domains change with the temporal progression of replication and transcription. Most likely the transcription occurring in a particular domain is transiently interrupted until the DNA in that domain is finished replicating. A dynamic underlying architecture is an appealing model for the basis of these spatial distinctions and genomic function [121,122].

Section 1.5. Statement of Hypothesis

The debate over whether or not actin is found in cell nuclei is over. Scientific interest now lies in what state nuclear actin is in, whether or not it plays structural roles, and its potential functions in nuclear processes. Most recently, FRAP experiments have shown that ~20% of nuclear actin is in a filamentous form [27] and the finding of numerous nuclear actin-binding proteins suggest actin dynamics are controlled [16]. There is also substantial evidence that actin may act as a local structure similar to the cytoskeleton. The predicted mechanism for maintaining discrete nuclear compartments, including chromatin domains, is through transient interactions with an underlying substructure. In relation to specific nuclear processes, it has been shown that polymerases are likely immobilized on a nuclear matrix, transcription factors are concentrated and attached to a matrix, and HATs and HDACs have matrix associations. The breadth of possible roles for actin in fundamental nuclear processes

is obviously large. Based on what is known of nuclear actin thus far, we propose to: disrupt F-actin so to achieve preliminary results on potential roles of actin in transcription and the phosphorylation of kinases and histone variants known to have roles in sensing DNA damage.

Chapter 2: Materials and Methods

Section 2.1. Reagents, and Antibodies

Latrunculin B was purchased from Calbiochem (Hornby, ON). Actinomycin D was purchased from Molecular Probes (Eugene, OR). 5-Fluorouridine, 4', 6-Diamidino-2 phenylindole (DAPI), 5,6-Dichlorobenzimidazole riboside (DRB), 1-(5-chloronapthalene-1-sulfonyl)-1H-Hexahydro-1, 4-diazepine (ML-9), 1-(5-isoquinolinesulfony)-2-methylpiperazine (H-7), and 2,3-Butanedione monoxime (BDM), were all purchased from Sigma (Oakville, ON). EDTA was purchased from the University of Alberta Biochemistry Stores (Edmonton, AB). Wortmannin was a gift of Drs. Razmik Mirzayans and Joan Turner (Edmonton, AB).

Antibody for fluorouridine (anti-BrdU) was purchased from Sigma (Oakville, ON). Antibody for γ-phosphorylated H2AX (anti-γH2AX) was a gift of Dr. Razmik Mirzayans and later purchased from Upstate (Lake Placid, NY). Antibody for phosphorylated ATM (anti-ATM phospho S1981) was purchase from AbCam (Cambridge, MA). Anti-mouse Alexa Fluor 488, anti-rabbit Alexa Fluor 488, and Alexa Fluor 546 phalloidin were purchased from Molecular Probes (Burlington, ON). Anti-rabbit cyanine Cy3 was purchased from Jackson ImmunoResearch Inc. (West Grove, PA).

Section 2.2. Cell Culture

10T1/2 cell line: Mouse embryonic cells were cultured at 37°C, 5% CO_2, in alpha modified minimal essential medium (αMEM) containing 10% fetal bovine serum (FBS) and 1% L-glutamine.

IM cell line: Indian muntjac skin fibroblast cells were cultured at 37°C, 5% CO_2, in Ham's F-10 media (F-10) containing 10% fetal bovine serum (FBS) and 1% L-glutamine.

HeLa cell line: Human cervical epithelial adenocarcinoma cells were cultured at 37°C, 5% CO_2, in Gibco culture media Dulbecco's modified Eagle's Media (DMEM) containing 10% fetal bovine serum (FBS) and 1% L-glutamine.

Raji cell lines: Human lymphoblast-like (B lymphocyte, Burkitt's lymphoma) cells were cultured at 37°C, 5% CO_2, in RPMI-1640 media (RPMI) containing 10% fetal bovine serum (FBS) and 1% L-glutamine.

AT2BE cell lines: Primary human fibroblast cells (ATM defective) were cultured at 37°C, 5% CO_2, in Ham's F12 medium containing 10% fetal bovine serum (FBS), 1% L-glutamine.

Section 2.3. Analysis on the effects of myosin inhibitors (ML-9, H-7, and BDM) and latrunculin on transcriptional competency

2.3.1. Fixed cell preparation and 5-fluorouridine labeling

All cells were maintained at subconfluent levels by regular passaging with an appropriate amount of trypsin (Gibco). One day prior to immunofluorescent labeling, approximately 35,000 cells were plated onto each 18 x 18 mm coverslips. The coverslips were then treated for 40 minutes with either 1 μM or 2 μM latrunculin A, 4 μM ML-9, 100 μM H-7, 20 mM BDM, or no-drug treatment control, followed by a 20 minute incubation with 15 μL of a 134 mM fluoruridine solution in 1mL of medium. The cells were then fixed for 10 minutes in a 4% (w/v) paraformaldehyde in PBS followed by three washes in PBS. Cells were permeabilized with PBS containing 0.5% (v/v) Triton X-100 for 10 minutes, followed by three washes in PBS. The cells were then incubated in 1° antibody (mouse BrdU) by inverting the coverslip on a 25 μl droplet of the antibody dilution (1:200 PBS) for one hour. The coverslips were then rinsed once with PBS containing 0.1% (v/v) Triton X-100 and three times with PBS. Cells were then incubated in a 25 μl droplet of 1:200 2° antibody (goat anti-mouse Alexa 488) and 1:500 dilution of phallodin for 1 hour. The coverslips were rinsed as before and mounted on slides containing 10μl of a 90% glycerol-PBS-based mounting medium containing 1mg of para-phenylene diamine/mL and 0.5 μg/mL of the DNA dye, DAPI (Sigma Prod. No.D9542). The slides were rinsed with

milli-Q water to remove any residual PBS crystals, which could negatively effect image acquisition. Slides were maintained at 4°C in the dark and images were acquired within one week.

2.3.2. Digital image microscopy for transcription

Two-dimensional images were taken with the Zeiss Axioplan 2 microscope with a 12-bit cooled Photometrics Sensicam CCD camera through the mid-section of cells. A 40X oil-immersion fluar lens (numerical aperture = 1.3) and three channels, DAPI, FITC/Alexa 488, and Cy3, were used to obtain a DNA image from the DAPI stain, a fluorouridine image from Alexa 488, and an actin image of the phallodin stain. All images within the same channel were taken at the same shutter speed so to maintain exposure times and image intensity. After collecting images of approximately 300 cells per condition, the images were analyzed using Metamorph Universal Imaging software.

2.3.3 Quantitative image microscopy for 5-fluorouridine labeling

Maintaining optimized settings as a constant throughout image acquisition allows for the signal intensities of individual nuclei to be characterized and quantitatively compared. Prior to image quantitation, the average background signal intensity was measured by randomly selecting background regions. Then, the average background intensity, plus two standard deviations, was subtracted from each

image resulting in the removal of background intensity from the images. Next, a binary nuclear mask was generated through signal intensity thresholding of the DAPI channel that was then applied to each of the channels to be quantified (e.g. DAPI, FITC/Alexa 488, Cy3). A variety of data, including total signal intensities and area for each nucleus, were measured and the raw data exported into Excel (Microsoft). Data were then compiled in Excel and exported into Prism version 3.03 (GraphPad) where all statistical analyses were performed.

2.3.4. Flow cytometry for 5-fluorouridine labeling

HeLa and Raji cells were subcultured to 65% confluency one day prior to experimentation. Control cells were left untreated whereas drug treated cells were incubated for one hour with either 200 μM latrunculin B, 50 μM latrunculin B, 75 μM DRB, or 4 μM actinomycin D. Following drug treatments all cells were incubated with 2 mM fluorouridine for an additional 20 minutes. The cells were harvested by treatment with EDTA and cell numbers were counted using a particle count and size analyzer (Becton Dickinson). They were then washed in PBS and spun at 400xg for 5 minutes. The cells were fixed in 1% paraformaldehyde at room temperature for 15 minutes. The paraformadehyde was removed and the cells were placed in 70% ethanol at -20°C overnight. The cells were spun and PBS washed before being placed in mouse monoclonal anti-BrdU antibody (Sigma) (1:500 PBS) or the mouse IgG1 (Sigma) (5μl/5x10^5cells) isotype control for 45 minutes on ice. The cells were washed in PBS and spun down before being returned to ice for 45

minutes in the goat anti-mouse Alexa 488 (1:300) secondary antibody. The cells were washed in PBS, spun, had their supernatant removed, and 1 mL of 60 μM propidium iodide (Sigma) solution was added for 30 minutes. The cells were washed in PBS and resuspended at $1x10^6$ cells/ml of PBS. Flow cytometry was preformed on a FACSort (Becton Dickinson) using Cell Quest version 3.2.1 fl (Becton Dickinson).

Section 2.4. Analysis of the effects of latrunculin treatment on histone γ-H2AX and ATM kinase phosphorylation

2.4.1. Fixed cell preparation and immunofluorescent labeling for γ-H2AX and phospho-ATM kinase

All cells were maintained at subconfluent levels by regular passaging with an appropriate amount of trypsin (Gibco). One day prior to immunofluorescent labeling, approximately 35,000 cells were plated onto each 18 x 18 mm coverslips and left to adhere overnight. The coverslips were then treated for 60 minutes with 20 μM wortmannin alone, or 40 minutes with 20 μM latrunculin B alone, or no-drug treatment controls. Some cells then received 5 Gy irradiation from a Shepard Irradiator so that for every drug treatment there was a corresponding irradiated coverslip and a non-irradiated coverslip. After irradiation the cells were incubated at 37°C for 15 minutes followed by fixation for 20 minutes in 4% (w/v) paraformaldehyde in PBS. After fixation the cells were washed three times in PBS followed by permeabilization with PBS containing 0.5% (v/v) Triton X-100 for 10

minutes. The cells were then washed three times in PBS and incubated in 1° antibody (mouse anti-γ-H2AX) by inverting the coverslip on a 25 μl droplet of the antibody mixture (1:5000 in PBS) for one hour. The 1° antibody rabbit anti-phospho ATM (1:500) was also used for an hour. The coverslips were then rinsed once with PBS containing 0.1% (v/v) Triton X-100 and three times with PBS. Cells were then incubated in a 25 μl droplet of 1:200 2° antibody (goat anti-mouse Alexa 488) for an hour. The 2° antibody for the phosphorylated ATM kinase was a 25 μl droplet of either 1:200 goat anti-rabbit Alexa 488, or 1:200 goat anti-rabbit Cy3. The coverslips were rinsed as before and mounted on slides containing 10 μl of a 90% glycerol-PBS-based mounting medium containing 1mg of para-phenylene diamine/mL and 0.5 μg/mL of the DNA dye, DAPI (Sigma Prod. No.D9542). The slides were rinsed with milli-Q water to remove any residual PBS crystals. Slides were maintained at 4°C in the dark and images were acquired within one week.

2.4.2 Digital image microscopy for γ-H2AX and phospho-ATM kinase

Two-dimensional images were taken with the Zeiss Axioplan 2 microscope with a 12-bit cooled Photometrics Sensicam CCD camera through the mid-section of cells. A 20X dry fluar lens (numerical aperture = 0.75) and three channels were used to obtain a DNA image of the DAPI stain, a γ-H2AX image using Alexa 488, and a phospho-ATM image using Alexa 488 or Cy3. All images within the same channel were taken at the same shutter speed so to maintain exposure times and image

intensity. After collecting images of approximately 100 cells per condition the images were analyzed using Metamorph Universal Imaging software.

2.4.3. Quantitative image microscopy of γ-H2AX and phospho-ATM kinase

Optimized settings were maintained throughout image acquisition to allow for quantitative comparison of the signal intensities of individual nuclei. Background subtraction and quantification were carried out as described in section 2.3.3.

2.4.4. Preparation of nuclei and protein acid-extraction for immunoblot analysis

Cell lines were grown at subconfluent levels on 15 cm tissue culture dishes. The medium was removed and cells were incubated with 0.53 mM EDTA until the cells became detached. Cells were collected and transferred to a 15 mL conical tube where they were pelleted by centrifugation at 1,500 RPM for 5 minutes and triturated with 10 mL PBS. Cells were washed an additional two times before being counted using a particle count and size analyzer (Becton Dickinson). The cells were pelleted at 1,500 RPM for 5 minutes before being resuspended with an appropriate volume of PBS so the final concentration of cells was 10×10^6 cells/mL.

The suspended cells were transferred to a sterile 1.5 mL plastic tube. Then the cells were lysed by resuspending in approximately 1ml of cold nuclei buffer (0.25M sucrose, 0.2M NaCl, 10 mM Tris/HCl pH8, 2 mM $MgCl_2$, 1 mM Ca Cl_2, 1% Triton X-100) containing freshly added 1 mM phenylmethanesulfonyl fluoride

(PMSF). Nuclei were harvested by centrifugation at 3,000xg for 1 minute and removal of the nuclei buffer.

To the tubes containing the equivalent of 10 x 10^6 nuclei, 570 µL of milli-Q water and 6.4 µL of concentrated sulfuric acid (H_2SO_4) were added, yielding a final concentration of 0.4N H_2SO_4. The samples were put on ice for 30 minutes to allow for acid solubilization of nuclear proteins. The nuclear proteins were clarified from nuclear debris by centrifugation at 14,000 RPM for 10 minutes at 4°C in the Eppendorf 5417R centrifuge. The supernatant was transferred to a clean 1.5 mL tube containing 60 µL of Tris buffer (pH 8.0). To this, 40 µL of 10N sodium hydroxide (NaOH) was added and mixed.

2.4.5. Gel Electrophoresis

The acid extracted samples were combined with a 1/3 total volume of 3x sample buffer (30 mL glycerol, 3.0 mL 2-mercaptoethanol, 6.0 g SDS, 2.28 g Tris, 1.5 mg bromophenol blue, pH to 6.8 with hydrochloric acid [HCl]) for SDS polyacrylamide gel electrophoresis (PAGE). The samples were boiled for 2 minutes and the equivalence of protein from 2 x 10^5 cells were loaded per lane on duplicate gels, one for antibody staining and one for Coomassie Blue staining. For analyzing acid extracted histones a 15% separating gel and a 5% stacking gel were used. For a 15% separating gel 2.5 mL of 4x separating buffer (1.5 M Tris, 0.4% SDS, pH to 8.7 with HCl) was added to 5 mL of 30% acrylamide (60.0 g acrylamide, 1.6 g bis-acrylamide, 200 mL H_2O), 2.5 mL H_2O, 10 µL TEMED, and 100 µL of 10%

ammonium persulfate. A 5% stacking gel was made by adding 1.5 mL of 4x stacking buffer (0.4 M Tris, 0.4% SDS, pH to 6.8 with HCl) to 1.0 mL of 30% acrylamide, 3.5 mL of H_2O, 6.0 µL of TEMED, and 60 µL of 10% ammonium persulfate. The gels were run in a Mini Protean III electrophoretic gel apparatus (Bio-Rad) at 85V, 140mA, and 250W for 20 minutes followed by 80 minutes at 158V, 140mA, and 250W, all in 1% running buffer (30g Tris Base, 10g SDS, 144g glycine in 10L H_2O). For primary identification, proteins were stained overnight at room temperature with Coomassie Blue (0.25 g Coomassie Brilliant Blue R250, 45 mL H_2O, 45 mL methanol, 10 mL glacial acetic acid). They were first destained in 25% methanol and 12.5% acetic acid for approximately 2 hours. They were further destained in a weak solution of 5% methanol and 7.5% acetic acid and stored in this solution. The gels were imaged with the AlphaImager gel documentation system equipped with AlphaEase version 3.3d software.

2.4.6. Immunoblotting and Development

Proteins were transferred to PVDF membranes using the Mini Protean III transfer system following the Bio-Rad protocol. Equivalent protein loading was confirmed by protein staining the PVDF membranes with copper phthalocyanine 3, 4', 4", 4'''-tetrasulfonic acid tetrasodium salt (CPTS). The membranes were incubated in 15 mL of CPTS for 30 minutes with gentle agitation at room temperature. Once the proteins were stained, the membrane was incubated in 50% (v/v) methanol in milli-Q water for 5 minutes to reduce the background. Images were

acquired with the AlphaImager gel documentation system equipped with AlphaEase version 3.3d software. The PVDF membranes were destained in PBS for 10 minutes. Once the bands disappeared, the membranes were blocked with 5% (w/v) non-fat milk in TBS containing 0.1% (v/v) Tween-20 (TBST) for 1 hour. The primary antibody, mouse monoclonal anti-γ-H2AX antibody (Trevigen), was used at a dilution of 1:5000. In a plastic bag, sealed on three sides, 1 mL of the antibody was added to the blot, and once all the air bubbles were removed the bag was sealed on the fourth side. Blots were incubated overnight at 4°C on a shaker. The following day, the blots received three 10-minute washes in TBST. Next, blots were incubated for 1 hour at room temperature with gentle agitation in the secondary antibody, anti-mouse horseradish peroxidase at 1:15,000 in 5% skim milk in TBST. Blots were washed three times in TBST before being inverted onto 500 μL of ECL plus, prepared as described by manufacturer, (Amersham Biosciences) and allowed to incubate for 5 minutes. Excess ECL plus was removed by dabbing the edge of the blot on a Kimwipe before being wrapped in a piece of Saran wrap. Blots were exposed to FujiFilm Super RX medical X-ray film for varying optimal lengths of time. Films were developed in a Kodak X-OMAT 2000A film processor.

2.4.7. Flow cytometry for γ-H2AX analysis

Adherent 10T1/2 cells were grown at subconfluent levels on 15 cm tissue culture dishes. Control cells were left untreated and drug treated cells received 20 μM latrunculin B for 40 minutes. There were duplicate plates for each condition so that

when half of the plates received 5 Gy irradiation from a Shepard Irradiator, the result was irradiated cells and non-irradiated cells for both control and drug treatments. After irradiation the cells were incubated at 37°C for 15 minutes, followed by a PBS rinse and addition of 3 mL of trypsin. Once cells had detached, they were collected, transferred into a 15 mL conical polyethylene centrifuge tube (Corning) and suspended in PBS. The cells were then spun down at 1,500 RPM in a Beckmann Accuspin FR centrifuge for 5 minutes and the supernatant was removed by aspiration. The cells were washed in PBS, followed by centrifugation at 1,500 RPM for 5 minutes. Cells were washed before being counted using a particle count and size analyzer (Becton Dickinson). The cells were pelleted at 1,500 RPM for 5 minutes and the supernatant removed. Cells were resuspended with an appropriate volume of PBS so that the final concentration of cells was 2 x 10^6 cells/mL. Subsequently, 1 mL aliquots were dispensed into 13 mL round-bottom polypropylene tubes (Starstedt), cells were pelleted again, and the supernatant removed. Cells were fixed and permeabilized through the slow addition and mixing of 70% ice-cold ethanol. Cells were stored at 4°C overnight before immunofluorescent labeling.

Prior to immunofluorescent staining, the 1 mL aliquots of ethanol-fixed cells were pelleted by centrifugation at 1,500 RPM for 5 minutes and the supernatant removed. Cells were resuspended in 5 mL of PBS, pelleted as before, and the supernatant removed. The cells were then placed in 75 μL of either mouse monoclonal anti-γ-H2AX antibody (Trevigen) (1:5000), or the mouse IgG1 (Sigma) isotype control (1:200) for 60 minutes on ice. The cells were washed in PBS and

spun down before being returned to ice for 60 minutes in 75 μL of the goat anti-mouse Alexa 488 (1:200) secondary antibody.

Following incubation with the secondary antibody, the cells were washed in 4 mL of PBS, centrifuged, and the supernatant removed. The cells were then resuspended in 1ml of PBS with 10μl RNase A, 30μl propidium iodide. The tubes were placed in a 37°C water bath for 30 minutes before the addition of 4 mL of PBS and centrifugation. The supernatant was removed and the cells were resuspended in a final volume of 500 μL and transferred to 4 mL Facsort tubes (Falcon). Samples were maintained in the dark and flow cytometry was conducted immediately. Flow cytometry was preformed on a FACSort (Becton Dickinson) using Cell Quest version 3.2.1 fl (Becton Dickinson).

Chapter 3. RESULTS. ELUCIDATING A ROLE FOR FILAMENTOUS ACTIN IN TRANSCRIPTIONAL PROCESSES

3.1. Chapter Introduction and Experimental Objectives

Chromatin Remodeling and Transcription

Nucleosomes are the basic structural units of chromatin organization and are comprised of approximately 146 base pairs wrapped twice around a histone octomer containing two of each of the histones H2A, H2B, H3, and H4 (Figure 3-1) [123]. A linker histone H1 stabilizes the structure and modulates the folding of chromatin into higher-order structures [124]. The degree of packaging of DNA is fundamental to regulating gene expression. Highly condensed DNA creates a barrier to interaction with transcriptional machinery and therefore changes in chromatin structure can alter gene expression by allowing for these interactions. Strategies to alleviate chromatin-mediated transcriptional repression include the action of ATP-dependent chromatin remodeling complexes and enzymes that modify histones. One highly conserved remodeling family is the multi-subunit SWI/SNF complex, which uses energy derived from ATP hydrolysis to alter nucleosome structure allowing for transcriptional machinery to access regions of DNA [125].

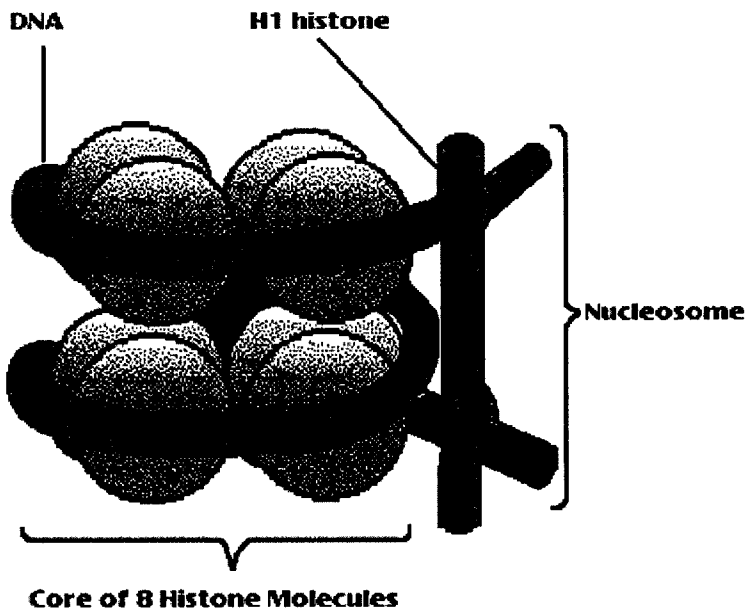

Figure 3-1. Schematic depiction of the nucleosome. The nucleosome consists of approximately 146 base pairs wrapped twice around an octamer of duplicates of the four core histones (H2A, H2B, H3, and H4). Histone H1 stabilizes the structure (modified from Kornberg, 1999) [123].

Actin was first found in the BAF complex, a mammalian homologue to yeast SWI/SNF, containing the highly related ATPases, hBRM and Brg 1[126]. Subsequently actin has been identified in other chromatin remodeling complexes including the *Drosophila* BAP complex, the yeast Ino80 complex, the mammalian p400 complex, NuA4 complex, and the TIP60 complex [127-131]. The exact role of actin in these complexes is unclear but there are indications that it has roles in ATPase activity and attachment to the nuclear matrix. Isolation of the mammalian BAF complex identified β-actin, an actin related protein (ARP) called BAF53, and nine other

proteins to be part of the complex [126]. Actin and BAF53 were found to be tightly associated with the ATPase Brg 1 and depolymerization of actin by latrunculin treatment inhibited ATPase activity [126]. When the BAF complex is examined in cell lines that do not express Brg 1 the complex lacks actin and BAF53 and does not associate with the nuclear matrix. An appealing model is that the site of attachment is to an actin-containing scaffold. When Brg 1 is expressed, the complex assembles and associates with the matrix indicating a potential function for actin in nuclear matrix attachment [126].

The presence of actin binding proteins in the nucleus allows for the possibility that signaling can be transmitted to chromatin remodeling complexes through changes in actin dynamics. Support for this idea comes from the *in vitro* finding that phosphatidylinositol 4,5-bisphosphate (PIP_2) which regulates actin binding proteins, causes association of BAF with the nuclear matrix [16]. Although there is no obvious connection between actin binding proteins and chromatin remodeling complexes the potential for regulating remodeling complexes via these proteins is intriguing. Whether or not actin has controlled polymerization in these complexes is yet to be determined.

Compartmentalization and Nuclear Territories

Modification of DNA and nucleosomes regulates gene expression; however there is also another level of transcriptional control, which is dependent on nuclear architecture and chromosome territories. Not only does the structural organization of

the individual chromosome effect gene expression but also the position of the chromosome in the nucleus is important. Chromosomal positioning seems to be determined in part by gene content [132]. One striking example is of the gene-poor chromosome 18 whose territories are found on the nuclear periphery whereas chromosome 19, which is approximately the same size as chromosome 18 but gene-rich, has territories found in the nuclear interior [133]. Another determinant of chromatin organization is related to differences in stages of replication; an example being that early and late replicating DNA occupies different foci with exclusive volumes [134]. There are many factors that can contribute to the compartmentalization of chromatin and interestingly some of the properties may be intrinsic to the chromatin itself.

It is possible that nuclear compartmentalization of chromatin is determined by chemical information contained within the genome. Although the question of how nuclear territories are determined is interesting, an equally fascinating question is: how do these non-membrane bound territories maintain their exclusive areas? Microscopy used to monitor the dynamics of nuclear compartments suggest that these domains may be maintained by physical structures [54]. More specifically a model of actin acting as a structure homologous to the cytoskeleton is particularly appealing. The importance of a physical nuclear architecture in transcription is supported by findings that transcriptionally inactive genes have A-T rich sequences that bind to a nuclear matrix allowing the transcriptionally active chromatin loops to be exposed and available to transcription factors and transcription machinery [101]. Actin may be part of the filamentous structure that chromatin attaches to and on which the large

multiprotein transcriptional machinery complexes assemble [135]. There are also reports of directed motion in the nucleus, which is an obvious candidate for facilitation by a nuclear motor-protein [136]. The recent finding of a nuclear myosin I isoform raises new mechanistic possibilities for compartmentalization especially when considering the common partnership of actin and myosin in the cytoplasm [137].

Nuclear Myosin I - in cooperation with actin as a molecular motor?

Antibodies to bovine adrenal myosin I (116kDa) recognize a 120kDa nuclear protein which has characteristics consistent with the myosin superfamily. Such characteristics are ATP binding, ATPase activity, and binding to actin in the absence, but not the presence, of ATP [137]. Further investigation has shown the protein to be a nuclear isoform of myosin I β (NMIβ) [138]. Sequence homology to the cytoplasmic myosin β I was >98% and differed by a unique 16-amino acid amino-terminal extension that is believed to direct it to the nucleus. A possible functional role for NMIβ in transcription comes from confocal and electron microscopy studies showing colocalization with RNA polymerase II (Pol II). Interestingly this colocalization was lost upon treatment with transcriptional inhibitors such as α-amanitin, responsible for the degradation of the large subunit of Pol II, and actinomycin D which binds to DNA. Furthermore, antibodies to the isoform coimmunoprecipitated with Pol II and inhibited RNA synthesis *in vitro*. Since NMIβ is an actin-dependent molecular motor it is suspected that it may power transcription by interacting with actin through its head region and cargo through its tail region. The finding of a nuclear actin-based

molecular motor raises many exciting possibilities for the organization and mechanics of nuclear processes.

Hypothesis

The discovery of actin in chromatin remodeling complexes suggests a role for actin in modulating transcription. Specifically, actin may have a role in ATPase activity and may be necessary for interactions with an underlying substructure that is possibly actin based. An underlying substructure could be important to chromosomal positioning. It is known that certain chromatin regions have attachments to the nuclear matrix and that this matrix could act as a scaffold for large transcriptional machinery to assemble and interact with transcriptionally active chromatin. It is speculated that this filamentous structure may be actin based and for this reason, as well as the fact that the actin-based molecular motor, NMIβ, is thought to have a role in transcription, we believe that the disruption of actin will result in the inhibition of transcription.

3.2. Changes in transcriptional activity in response to the disruption of actin myosin interactions

NMIβ may facilitate transcription through interactions with actin and therefore drugs that inhibit myosin-actin interactions can be useful. Two such drugs are H-7 and ML-9, which are myosin light chain kinase (MLCK) inhibitors that

interfere with the ATP-binding site of the kinase molecule [139]. ML-9 and H-7 can affect other enzymes such as camp-dependent protein kinase (PKA) and protein kinase C (PKC) but at different concentrations. ML-9 inhibits MLCK at a K_I (concentration of the competing ligand that will bind to half the binding sites at equilibrium) of 3.8 μM, and inhibits PKA and PKC at a K_I of 32 μM and 54 μM, respectively [140]. H-7 inhibits MLCK at a K_I of 97 μM, and inhibits PKA and PKC at a K_I of 3 μM and 6 μM, respectively [140]. For this reason, the concentrations of 4 μM for ML-9 and 100 μM for H-7 were used in the following experiments.

10T1/2, IM, and HeLa cells received treatments with either of the MLCK inhibitors, ML-9 or H-7, followed by incubation with fluorouridine, a halogenated nucleoside, which incorporates into newly transcribing RNA in place of endogenous uridine. The cells were then fixed and stained with anti-bromodeoxyuridine, which recognizes fluorouridine, and DAPI, which stains DNA. 2-dimensional images can then be collected and analyzed. It is important that while collecting images the same exposure times are maintained. This allows for direct quantitative comparison between the images. The images are quantified using Universal Imaging Metamorph software. To do this, a threshold is applied to the DAPI images to create a binary mask that defines the area of the nucleus. The mask is then used to define the cellular regions where fluorouridine intensity is measured to determine amounts of transcriptional activity.

Both H-7 and ML-9 drug treatments result in a disruption of transcription as indicated by the reduced amount of fluorouridine incorporation (Figure 3-2 and 3-3). H-7 is more effective with a reduction in fluorouridine incorporation by almost 86%

in comparison to the control whereas ML-9 only shows a reduction by approximately 40% in comparison to its control. As seen in Figure 3-4, even the less efficacious ML-9 treatment has an obvious effect on transcriptional activity, most notably the lack of bright nucleoli indicating a deficiency in RNA polymerase I transcription.

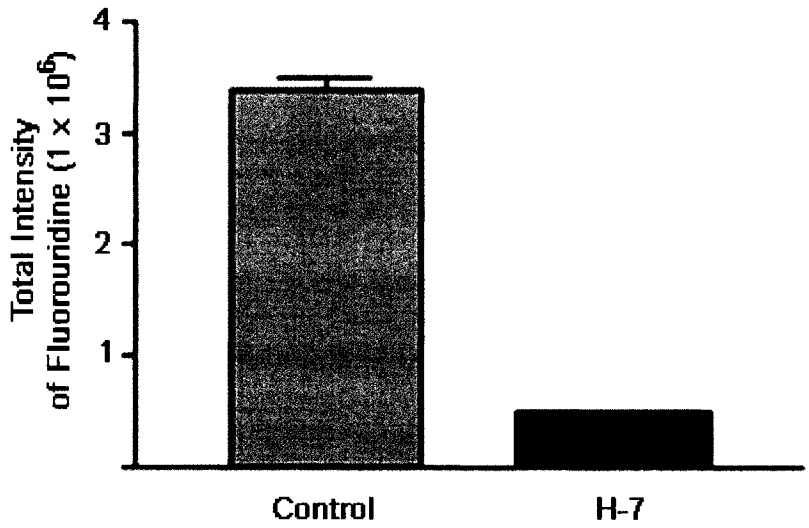

Figure 3-2. Interfering with the ATP-binding site of myosin light chain kinase reduces transcriptional activity as shown by the effects of H-7. 10T1/2 cells were treated with 100 μM H-7 for 40 minutes followed by a 20-minute incubation with 2 mM fluorouridine. The result shown is representative of multiple experimental replicates.

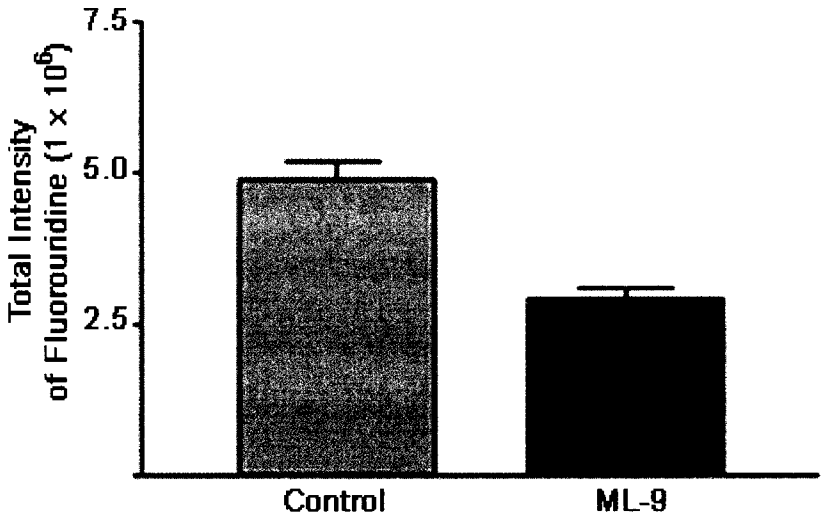

Figure 3-3. Interfering with the ATP-binding site of myosin light chain kinase reduces transcriptional activity as shown by the effects of ML-9. 10T1/2 cells were treated with 4 μM ML-9 for 40 minutes followed by a 20-minute incubation with 2 mM fluorouridine. The result shown is representative of multiple experimental replicates.

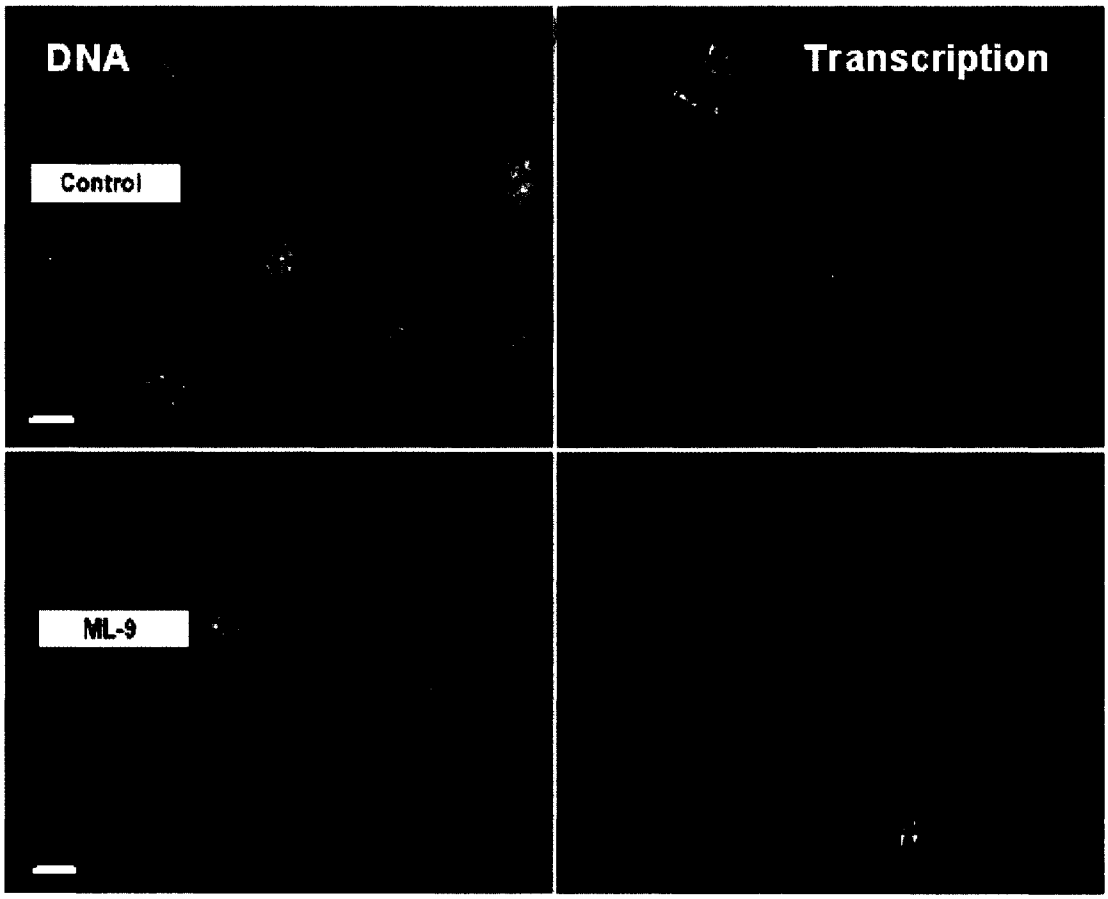

Figure 3-4. Disruption of actin-based myosin molecular motors inhibits transcription as seen by microscopy images. The left panel shows the nuclei of control (top panel) and ML-9 treated (bottom panel) 10T1/2 cells. The right panel represents fluorouridine incorporation into newly synthesizing RNA detected by an anti-bromodeoxyuridine monoclonal antibody that recognizes halogenated nucleotides. The arrows indicate nucleoli representing RNA polymerase I transcription. The intensity of this signal is dramatically reduced in ML-9 treated cells as seen in the bottom panel. A 40X oil-immersion fluar lens (numerical aperture = 1.3) was used to obtain images. The scale bars represent 10 μm.

Although ML-9 was not the MLCK inhibitor that was the most effective in disrupting transcription it did show further reduction in the amount of transcriptional activity when administered for increasingly longer periods of time (Figure 3-5).

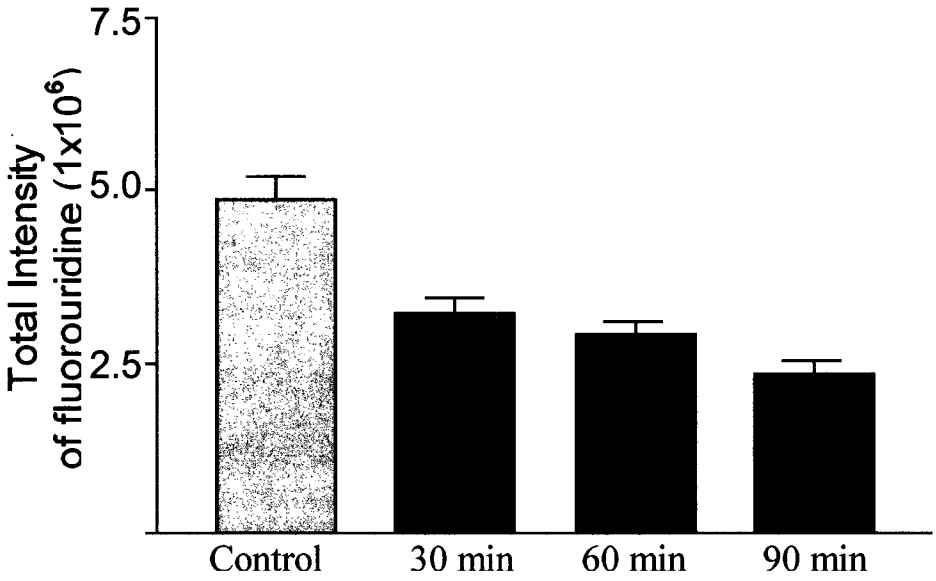

Figure 3-5. Increasing time treatments with ML-9 causes corresponding decreases in transcriptional activity. 10T1/2 cells received 4 μM ML-9 treatments followed by a 20-minute incubation with 2 mM fluorouridine. The result shown is representative of three experiments.

2,3-butanedione monoxime (BDM) had been found to act as a general myosin inhibitor that directly disrupts actin-myosin interactions by inhibiting myosin ATPase activity with low affinity [141]. To supplement the previous findings BDM was used in an analogous manner to ML-9 and H-7 prior to incubation with flurouridine. The reduction of fluorouridine incorporation was approximately 81% in comparison to the non-drug treated control (Figure 3-6). A comparison of the reduction in incorporation of fluorouridine as a result of the different myosin inhibitors is shown in Table 3-1.

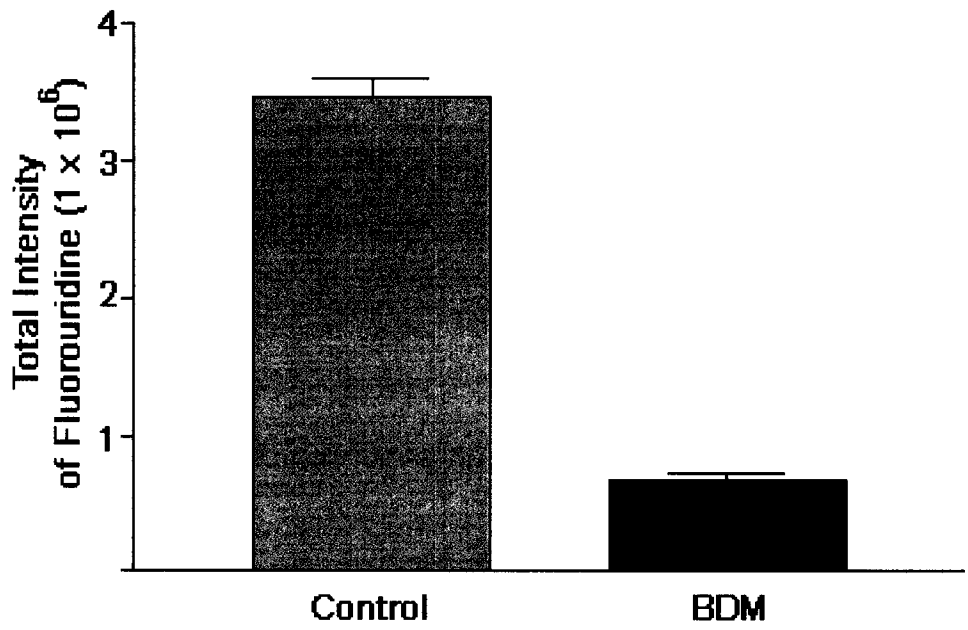

Figure 3-6. A general myosin inhibitor reduces transcription as shown by the effects of BDM. 10T1/2 cells received 20 mM BDM followed by a 20-minute incubation with 2 mM fluorouridine. The result shown is representative of multiple experimental replicates.

Controls (Separate Experiments)	Total Intensity Mean ± SEM ($1x10^6$)	Drug	Total Intensity Mean ± SEM ($1x10^6$)	Ratio of difference (Control/Drug)
Non-ML-9 treated	4.849 ± 0.350	ML-9	2.886 ± 0.190	1.68
Non-H-7 treated	3.373 ± 0.133	H-7	0.489 ± 0.015	6.87
Non-BDM treated	3.465 ± 0.132	BDM	0.678 ± 0.047	5.11

Table 3-1. Inhibitors of myosin actin interactions result in decreases in transcriptional activity. All treatments are in10T1/2 cells.

3.3. Changes in transcriptional activity in response to the disruption of actin filaments

Actin may function in transcription as part of a myosin-actin molecular motor however; the presence of actin in chromatin remodeling complexes indicates other potential roles [126]. One such role may be, F-actin in remodeling complexes is necessary for decondensing regions to be transcribed. By directly inhibiting actin, both myosin interactions as well as functions in remodeling complexes can be inhibited. A commonly used drug that disrupts F-actin is latrunculin, which binds and sequesters actin monomers. This interrupts the treadmilling process where the loss of monomers from one end of the filament is countered by replacing the monomers at the other end. Consequently the overall result of latrunculin treatments is a decrease in the amount of actin filaments.

10T1/2 and HeLa cells received a forty-minute drug treatment of either 1μM or 2 μM of latrunculin A. These doses allow the cells to remain adherent to the coverslips while the majority of F-actin is disrupted as observed by the rounded cell shape and phalloidin staining. The cells were then incubated with 2 mM fluorouridine for twenty minutes, followed by fixation and staining with anti-bromodeoxyuridine for the fluorouridine stain, DAPI to stain the DNA, and phalloidin to stain the actin. 2-dimensional images are collected and quantified using Universal Imaging Metamorph software.

The results show a large decrease in the amount of transcriptional activity as a result of latrunculin A treatments (Figure 3-7). Quantification shows treatments of 1

μM latrunculin A to reduce the levels of transcription by almost 80% and treatments of 2 μM latrunculin A reduce levels by over 85% when compared to the non-drug treated control cells. More specifically, RNA polymerase I transcription was almost completely eliminated as seen by the absence of nucleolar staining in latrunculin treated cells (Figure 3-8). As well, there is a reduction in the intensity of the nucleoplasm in response to latrunculin treatments indicating a disruption of RNA polymerase II transcription (Figure 3-8).

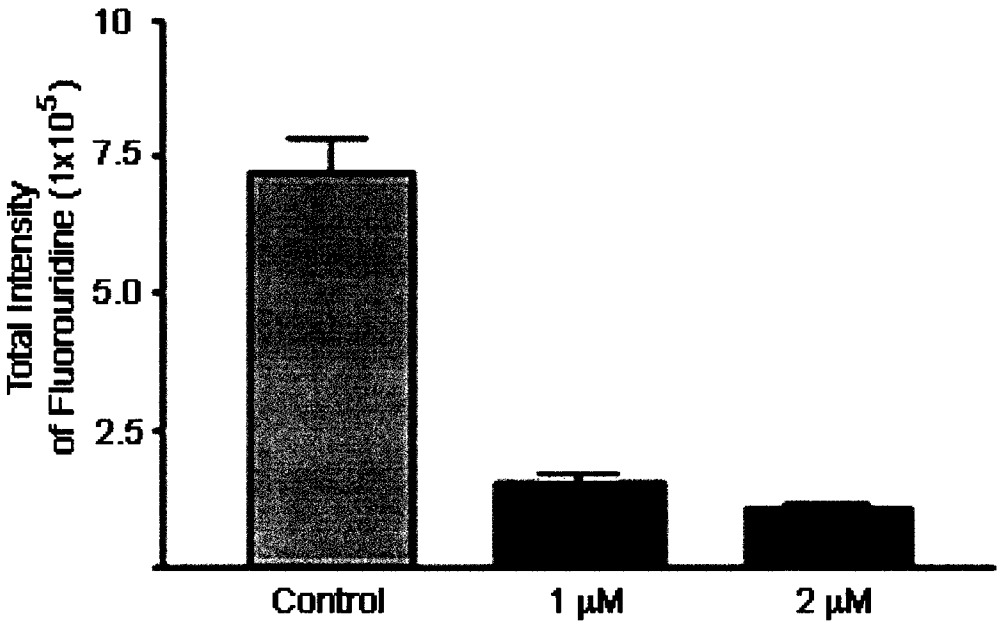

Figure 3-7. Disruption of F-actin by 1 μM and 2 μM latrunculin A treatments result in an inhibition of transcription. 10T1/2 cells were treated with either 1 μM or 2 μM of latrunculin A for 40 minutes followed by a 20-minute incubation with 2 mM fluorouridine. The result shown is representative of multiple experimental replicates.

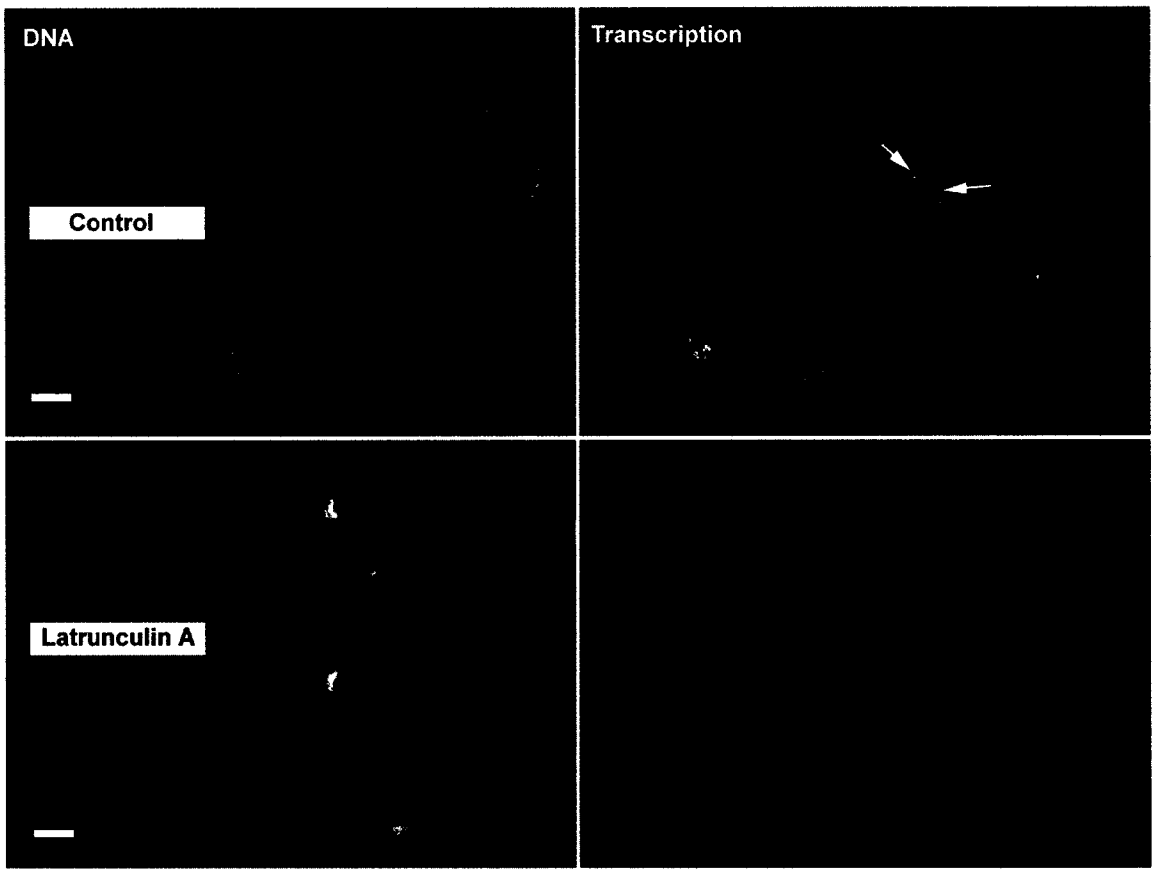

Figure 3-8. Disruption of F-actin inhibits transcription as seen by microscopy images. The left panel shows the nuclei of control (top panel) and latrunculin A treated (bottom panel) 10T1/2 cells. The right panel represents fluorouridine incorporation into newly synthesizing RNA detected by an anti-bromodeoxyuridine monoclonal antibody that recognizes halogenated nucleotides. The arrows in the top panel indicate nucleoli with high levels of transcription. The intensity of the signal is dramatically reduced in latrunculin A treated cells as seen in the bottom panel. A 40X oil-immersion fluar lens (numerical aperture = 1.3) was used to obtain images. The scale bars represent 10 μm.

3.4. Changes in transcriptional activity are independent of shape change

Latrunculin inhibits both the cytoplasmic and nuclear actin pools. The obvious criticism is that latrunculin treatments disrupt the actin cytoskeleton causing changes in cell shape. To determine if the reduction in levels of transcription are the result of these shape changes both an adherent HeLa cell line, and a suspension Raji cell line, received drug treatments, followed by fluorouridine incorporation, fixation, and analysis by flow cytometry. Control cells were untreated and drug treated cells received either: 50 μM latrunculin B, 200 μM latrunculin B, or 75 μM 5,6-Dichlorobenzimidazole riboside (DRB) with 4μM actinomycin D. DRB and actinomycin D are transcriptional inhibitors of RNA polymerase II and RNA polymerase I, respectively, and are useful as positive controls for transcriptional inhibition. It is important to acknowledge the apparent inconsistency in latrunculin concentrations between this experiment and the previous one. The higher dose of latrunculin B (50 μM or 200 μM versus 1 μM or 2 μM of latrunculin A) is necessary due to the relative weakness of latrunculin B in comparison to latrunculin A. Latrunculin B is now used instead of latrunculin A due to cost considerations. All drug treatments were sixty minutes followed by an additional twenty-minute incubation with 2 mM fluorouridine. The cells were then fixed and stained with anti-bromodeoxyuridine, which recognizes fluorouridine, and propidium iodide that stains double stranded DNA.

The Raji suspension cells incorporate less fluorouridine in response to latrunculin B treatments (Figure 3-9).

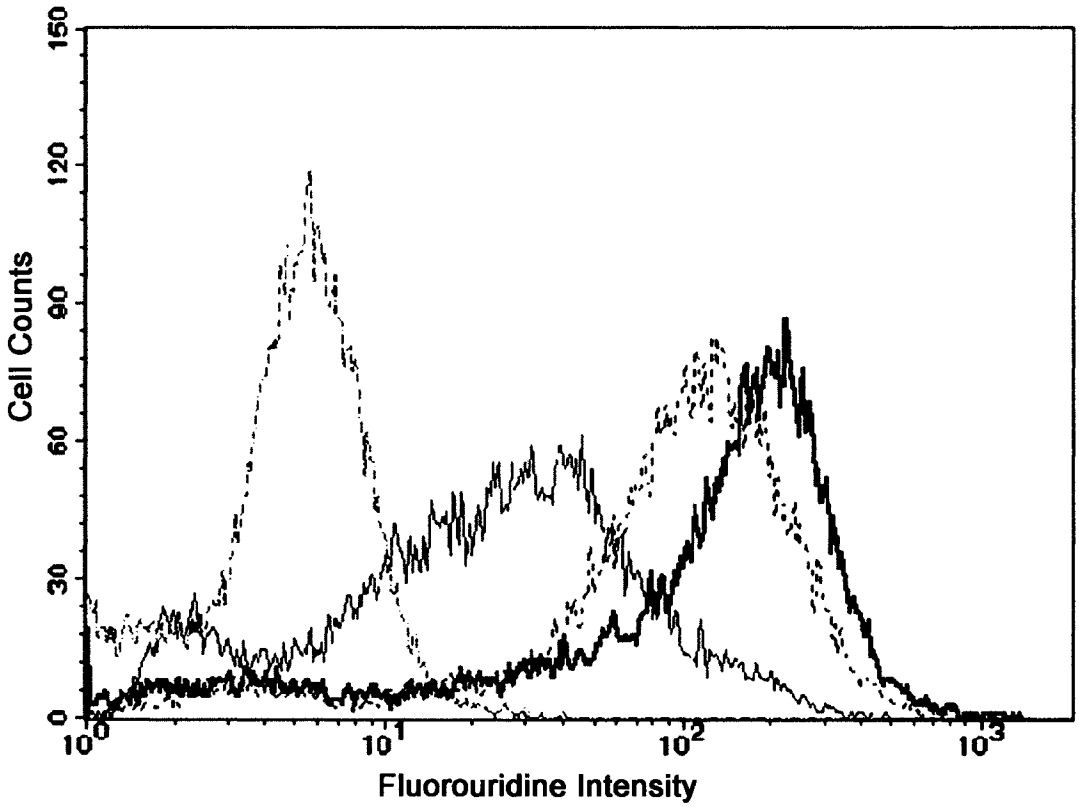

Figure 3-9. Disruption of F-actin causes a decrease in transcriptional activity in suspension cells as shown by flow cytometry. The red line represents control Raji cells treated with the transcriptional inhibitors actionmycin D and DRB. A 200 μM latrunculin B treatment is represented by the blue line and has a reduced amount of fluorouridine incorporation, as does the 50 μM latrunculin B treatment represented by the green line. The black line is furthest to the right and represents untreated control cells. All treatments are in Raji suspension cells. A representative result is shown. Experiment was performed in triplicate. (Christi Andrin)

The x-axis represents the intensity of the fluorouridine signal for the given count of cells shown on the y-axis. The line furthest to the right represents non-drug treated cells and therefore the highest amount of transcriptional activity as seen by the mean intensity of fluorouridine incorporation being over 160. The green line represents cells treated with 50 μM latrunculin, and with a mean intensity of 124.74 the reduction in comparison to the control cells is approximately 24%. 200 μM latrunuclin B treatments are represented by the blue line in the center of the graph and show an even larger reduction in fluorouridine incorporation, with a mean intensity of 42.26 and a percent reduction around 74%. Finally, the red line represents cells treated with the transcription inhibiting drugs actionomycin D and DRB. These cells have the least amount of fluorouridine incorporation with the mean intensity of only 7.17 and a reduction around 96%. The results can be compared to those found in adherent cell lines (Figure 10).

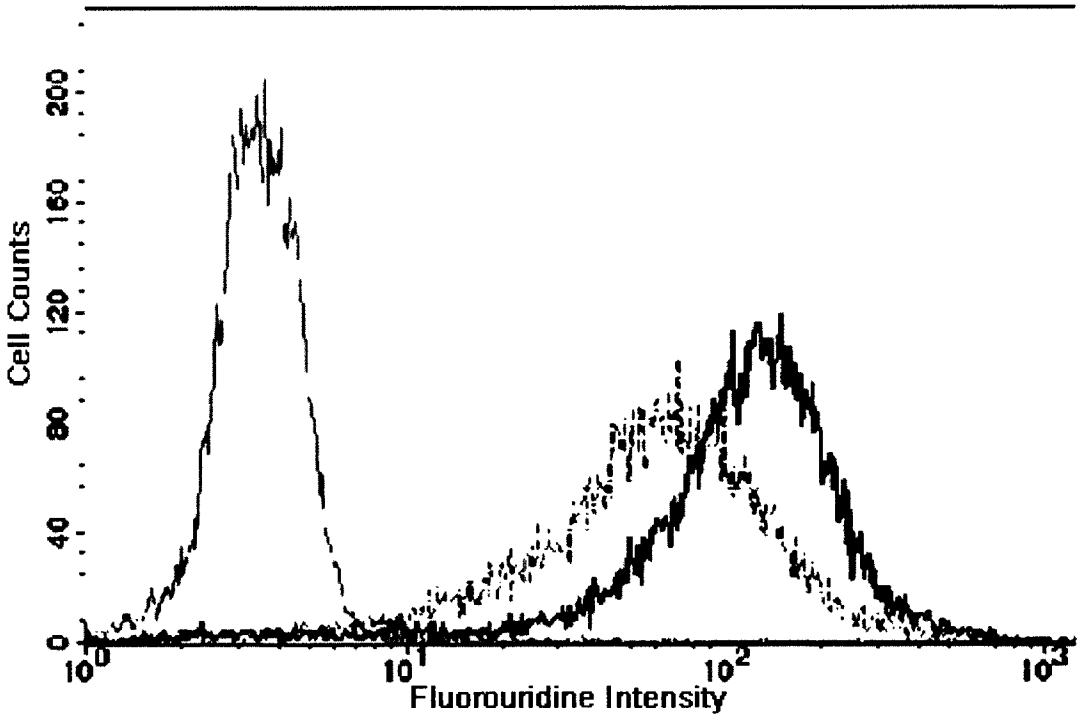

Figure 3-10. Disruption of F-actin causes a decrease in transcriptional activity in adherent cells as shown by flow cytometry. The blue line represents control HeLa cells treated with the transcriptional inhibitors actinomycin D and DRB. A 200 μM latrunculin B treatment is represented by the red line and has a reduced amount of fluorouridine incorporation. The black line represents untreated control cells. All treatments are in adherent HeLa cells. A representative result is shown. Experiment was performed in triplicate. (Christi Andrin).

The line with the highest amount of transcriptional activity is that on the right that represents non-drug treated cells with a mean intensity of 134.71. The 200 μM latrunculin B treatment is represented by the red line and has a mean intensity of 76.36 and therefore a reduction in transcriptional activity of around 43% when compared to the control cells. The cells treated with the transcriptional inhibitors actinomycin D and DRB show the lowest levels of transcriptional activity with a mean intensity of 6.8 and a percent reduction around 95%. Taken together these results show that both the Raji suspension cells and the adherent HeLa cells have an inhibition in transcriptional activity in response to latrunculin B treatments. The reduction in fluorouridine incorporation in response to 200 μM latrunculin B is larger in Raji cells than in HeLa cells. Perhaps the Raji cells are more sensitive to latrunculin treatments due to an increase in the amount of surface area exposed to the drug. Regardless, the response to latrunculin treatments in both suspension and adherent cells demonstrates that the reduction in transcription is not a response to a general shape change.

3.5. Chapter Summary

More than twenty years ago nuclear actin was suspected to play a fundmental role in transcription due to the finding that actin antibodies injected into *Xenopus* oocytes inhibit transcription of lampbrush chromosomes [142]. The presence of actin in numerous chromatin remodeling complexes, as well as its apparent necessity for the proper assembly of these complexes, suggests an important role for actin in the

function of chromatin remodeling complexes. Some possibilities include actin as, an exchange factor for the ATPase, mediator of localization of the complex, or perhaps regulator of the complex in response to signaling. The finding of numerous actin-binding proteins in the nucleus suggests that actin polymerization and dynamics could be controlled in chromatin remodeling complexes [126]. The proper functioning of remodeling complexes is important in decondensing areas of DNA to be transcribed. In fact the RNA polymerase II complex has been shown to include a chromatin remodeling complex [143]. The decrease in transcriptional competency as a result of F-actin disruption may be due to a requirement for F-actin in chromatin remodeling.

The maintenance of proper compartmentalization may also mediate transcription. Actin as a component of nuclear structure could be necessary for the assembly of transcriptional machinery with DNA. Support for this comes from findings that actively transcribed genes as well as chromatin rich in acetylated histones, which are thought to be markers for active transcription, are found enriched in the nuclear matrix fraction [101]. The disruption of F-actin may cause the disassembly of a local structure necessary for the proper functioning of transcriptional machinery. Furthermore, the presence of a nuclear myosin I isoform and its associations with the RNA polymerase II complex suggest an actin-based molecular motor may act in transcriptional processes. The effectiveness of MLCK inhibitors seems to vary and more recently doubts have been raised about the efficacy of BDM as a general myosin inhibitor since the ATPase activity in some classes of myosins remained unchanged despite BDM treatments [144]. However, the large reduction in

transcriptional activity in response to these inhibitors is an interesting preliminary result suggesting roles for myosin-actin interactions in transcription.

Chapter 4: RESULTS. ELUCIDATING A ROLE FOR FILAMENTOUS ACTIN IN REPAIR PROCESSES

Section 4.1. Chapter Introduction and Experimental Objectives

DNA double strand breaks (DSBs) can be generated by ionizing radiation and are considered to be amongst the most serious DNA lesions. To maintain cellular integrity these breaks must be recognized and repaired through mechanisms such as non-homologous end-joining (NHEJ) or homologous recombination (HR) [9,145]. In cases where repair is not possible, cells enter apoptosis thus preventing the propagation of errors. However, not all DSBs are the result of damage, some are required for steps in meiotic and V(D)J (variable, diversity, joining) recombination. A commonality in all these scenarios is that the break site must be recognized before it can be dealt with. The question remains: how does the cell recognize sites of DNA DSBs? One potential mechanism is the γ-phosphorylation of histone H2AX, yielding the modified γ-H2AX, at the sites of DNA breaks [146].

H2AX is Phosphorylated in Response to Double Strand Breaks

H2AX is a highly conserved variant of the nucleosomal histone family H2A. Peptide mapping and cDNA analysis have shown the carboxyl-terminal region of H2AX differs from the bulk H2A species by length as well as a conserved serine, glutamine (SQ) motif that has an invariant position [147]. This motif is conserved in H2AX homologs

throughout evolution, indicating an important function, potentially the γ- phosphorylation of the serine residue in response to DNA DSBs [148]. The foci that form in response to ionizing irradiation contain hundreds to several thousand γ-H2AX molecules. In many mammalian and mouse cells H2AX phosphorylation reaches half-maximal amount in 1-3 minute after irradiation and continues to increase over the first 30 minutes [146]. γ-H2AX not only responds to breaks inflicted by DNA damage but also those created in recombination and apoptosis [149,150].

V(D)J rearrangements are recombination events that require DSBs to create a plethora of gene products for the immune system [151]. The breaks are induced between the immunoglobin and T cell receptor coding gene segments by recombination activating gene (RAG) protein [149]. Although it had been presumed that the broken DNA was sequestered from the DNA damage sensing pathways, Chen *et al.* found that γ-H2AX foci are formed at the sites of V(D)J recombination induced DSBs [149]. This finding marks the first evidence of DNA damage surveillance machinery being used in V(D)J recombination. However it is still unclear as to how γ-H2AX coordinates the sensing and signaling pathways in response to DSB since γ-H2AX is not necessary for V(D)J joining or recombination [152]. γ-H2AX foci formation is also seen in response to DNA breaks inflicted during apoptosis. Apoptosis is in part characterized by chromatin condensation and fragmentation of the cell into apoptotic bodies that are reabsorbed by the organism [7]. γ-H2AX foci form about 1 hour after apoptotic pathways are initiated consistent with when DSBs are detected [150]. The function of γ-H2AX at these sites is not known however; one

can speculate that they mark the site of damage to recruit nucleases. This is similar to the better-known role of γ-H2AX in repair pathways and more specifically, its potential role in recruitment of repair proteins to sites of DNA damage.

γ-H2AX Colocalizes with Repair Proteins

The main kinase to phosphorylate H2AX is ataxia telangiectasia mutated (ATM), a phosphatidylinositol 3-kinase protein kinase-like (PIKK), with low levels of H2AX phosphorylation being accomplished by another PIKK called, DNA dependent protein kinase (DNA-PK) [153]. Prior to irradiation ATM is inactive and associated in dimers with the kinase region of one monomer bound to serine 1981 of another monomer. Upon irradiation ATM is activated by rapid intermolecular autophosphorylation of serine 1981. Evidence of activation of ATM in the presence of very few DNA breaks suggests that autophosphorylation is induced by changes in chromatin structure rather than direct binding to DNA breaks [154]. There is evidence of a role for ATM and γ-H2AX in the formation of repair foci at the sites of DSBs [153]. Paull *et al.* found the repair factors Rad 50 and Rad 51, which are important in HR, each independently colocalize with γ-H2AX in response to DNA damage, as does the product of the BRCA1 tumor suppressor gene [155]. Further support for the importance of H2AX in aiding the assembly of repair complexes comes from studies using H2AX deficient mice. H2AX-/- mice have chromosomal instability, repair defects, and show a decrease in the recruitment of Nijmegen breakage syndrome protein (NBS1), the p53 binding protein 1 (53BP1), and BRCA1 into repair foci [156]. Other studies using laser scissors and

ionizing radiation, two methods for inflicting DSBs, show that BRCA1 is recruited earlier than both Rad50 and Rad51, and that inhibiting γ-phosphorylation of H2AX also interferes with focus formation [155]. It was surprising that BRCA1 assembly is upstream from the other repair proteins since BRCA1 lacks DNA binding capabilities and other DNA-binding proteins such as Rad51 were thought to recruit BRCA1. However, when examining the mechanism of binding between γ-H2AX and other proteins, it is possible to consider BRCA1 binding directly to γ-H2AX instead of to DNA.

NBS1 was found to interact directly with γ-H2AX rather than with DNA, providing a suitable example for γ-H2AX recruitment of proteins through binding [157]. While the NBS1 has no DNA binding region it does contain a combination of a fork-head associated (FHA) domain and the BRCA1 C-terminal domains (BRCT) through which it interacts with γ-H2AX. NBS1 lacking the FHA/BRCT domain is unable to interact with γ-H2AX whereas recombinant FHA/BRCT domains alone can interact with γ-H2AX [157]. Other proteins that possess BRCT domains and have been found to colocalize with γ-H2AX include, BRCA1, and 53BP1 [155,158]. Furthermore, many other proteins involved in cell cycle control, recombination, and DNA repair contain BRCT motifs and could potentially utilize them for interactions with γ-H2AX.

Changes in Chromatin Structure

DNA DSBs and the phosphorylation of H2AX may make the break site more accessible and/or may cause changes that facilitate the recruitment of proteins. One

view, the "histone code" hypothesis, sees distinct modifications to histones as a language that is read by other proteins [159]. Thus, phosphorylation of H2AX at the particular serine residue could serve as a code to recruit proteins containing a particular interacting domain, perhaps those with BRCT motifs. Another possibility, involves the post-translational modification of histone tails, which elicit changes in higher-order chromatin structure. It is well known that histone modifications can mediate important nuclear processes including transcription and repair [160]. A common example is the post-translational modifications of core histones including their acetylation, phosphorylation, methylation, ubiquitination, glycosylation, and ADP-ribosylation [160]. In particular, histone tail acetylation has been shown to mediate histone-DNA and histone-histone interactions between adjacent nucleosomes and nucleosomes contained in other fibers [159]. Intuitively, highly condensed chromatin is antagonistic to processes such as gene expression while less condensed chromatin is amenable to gene expression. Histone acetylation can change the level of compaction by disrupting histone-tail interactions thus promoting expression. In an analogous manner, phosphorylation of H2AX could create a change in chromatin structure that facilitates repair processes.

Changes to chromatin structure may be necessary in certain processes that deal with DSBs. For example, chromatin expands and contracts during stages of synaptonemal complex (SC) formation, a meiosis specific structure formed between homologs [161]. Recombination, through programmed DSBs, precedes and is required for the formation of SC. H2AX phosphorylation is shown to also precede initiation of SC formation and coincides with zygotene, a chromatin compaction stage

necessary for SC formation [161]. It is suspected that phosphorylation and dephosphorylation of H2AX may cause phases of chromatin compaction and expansion that are necessary for meiotic recombination.

Chromatin diversity is in part generated by different variants of histones comprising the nucleosomes. It is not clear why H2AX serves as a unique marker for DNA DSBs, however the presence of the conserved SQ motif provides several possibilities. In light of the 'histone code hypothesis' the phosphorylation of the conserved serine residue in H2AX may serve as a signal for the recruitment of repair proteins to the site of DNA DSBs. On the other hand, phosphorylation of H2AX could act in a manner analogous to acetylation of histone tails. A change in chromatin structure at the site of the break could enhance the recognition of the break site, as well as increase the recruitment of repair proteins and thus facilitate the repair process. Future investigations will be sure to elucidate whether or not the common initial response of γ-H2AX foci formation due to DNA DSBs corresponds to universal changes in chromatin structure.

Hypothesis

F-actin may play an important structural role in nuclear architecture and therefore may mediate the phosphorylation of H2AX. More specifically, changes in nuclear architecture could effect the activation of ATM and thus change levels of H2AX phosphorylation. For example, the disruption of F-actin could lead to a change in nuclear organization that results in the dissociation, autophosphorylation,

and activation of ATM, consequently, an increase in γ-phosphorylation of H2AX in response to F-actin disruption could be expected even in the absence of DNA damage.

Section 4.2. Changes in H2AX γ-phosphorylation in response to disruption of filamentous actin

Cells were treated with latrunculin B, which prevents actin polymerization, to determine if the disruption of F-actin increases the γ-phosphorylation of histone H2AX. 10T1/2 cells cultured on coverslips were treated with either 20 μM latrunculin B for 40 minutes or no drug treatment and received either 5 Gy irradiation or no irradiation. The cells were then incubated post-irradiation for fifteen minutes to allow for H2AX phosphorylation, followed by fixation and fluorescent antibody staining. Slides were imaged and quantified. Analysis of the total intensity of the Alexa 488 signal shows a decrease in γ-phosphorylation of H2AX in latrunculin B treated cells, both with and without irradiation (Figure 4-1). Cells irradiated under control conditions have a mean total intensity of 14.84×10^5 (N=271) and the irradiated latrunculin treated cells have a mean intensity of 8.269×10^5 (N=326) (Table 4-1). Using a two-tailed P value and a 95% confidence interval for an unpaired t-test these differences are considered to be extremely statistically significant (P value <0.0001). Furthermore, non-irradiated control cells and non-irradiated latrunculin treated cells were also found to have a statistically significant (P value <0.0001) difference in the basal levels of γ-H2AX. The mean intensity of the

non-irradiated non-drug treated cells is 3.89 x 10^5 (N=186) whereas the mean intensity of the non-irradiated latrunculin cells is 2.84 x 10^5 (N=286).

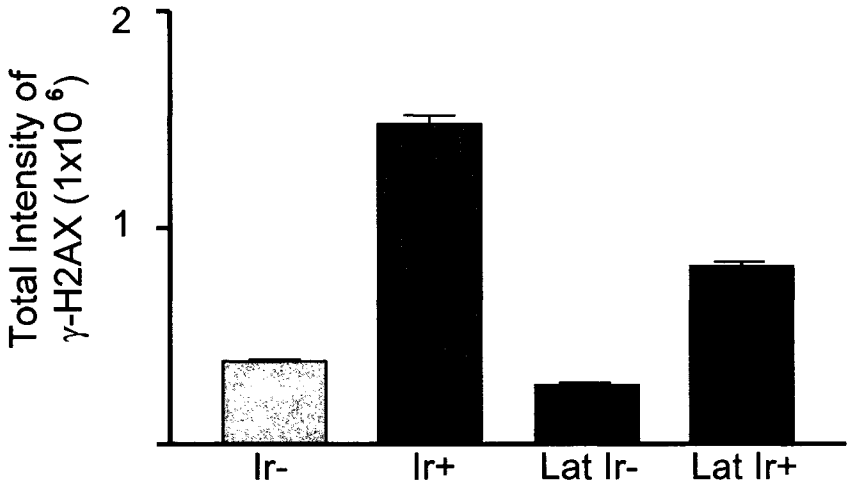

Figure 4-1. Disruption of F-actin causes a decrease in γ-H2AX as found by immunofluorescence microscopy. 10T1/2 cells were treated with 20 μM latrunculin B for 40 minutes. The result shown is representative of multiple experimental replicates.

Condition	**Total Intensity Mean ± SEM** (1 x 10^5)	N
Ir-	3.8900 ± 0.1699	186
Ir+	14.8400 ± 0.3823	271
Lat Ir-	2.8450 ± 0.1010	286
Lat Ir+	8.2690 ± 0.2421	326

Table 4-1. Irradiation and the disruption of F-actin cause differences in H2AX phosphorylation as seen by immunofluorescence.

Section 4.2.1. Does imaging using fluorescence microscopy falsely detect changes in H2AX phosphorylation due to differences in cell shape?

The differences in γ-H2AX intensity between control cells and latrunculin treated cells are difficult to determine by visual inspection alone because the disruption of the actin cytoskeleton causes the cells to round up. As a result, rounded latrunculin treated cells appear to have more intense signal since the three-dimensional information is projected into a two-dimensional dataset (Figure 4-2).

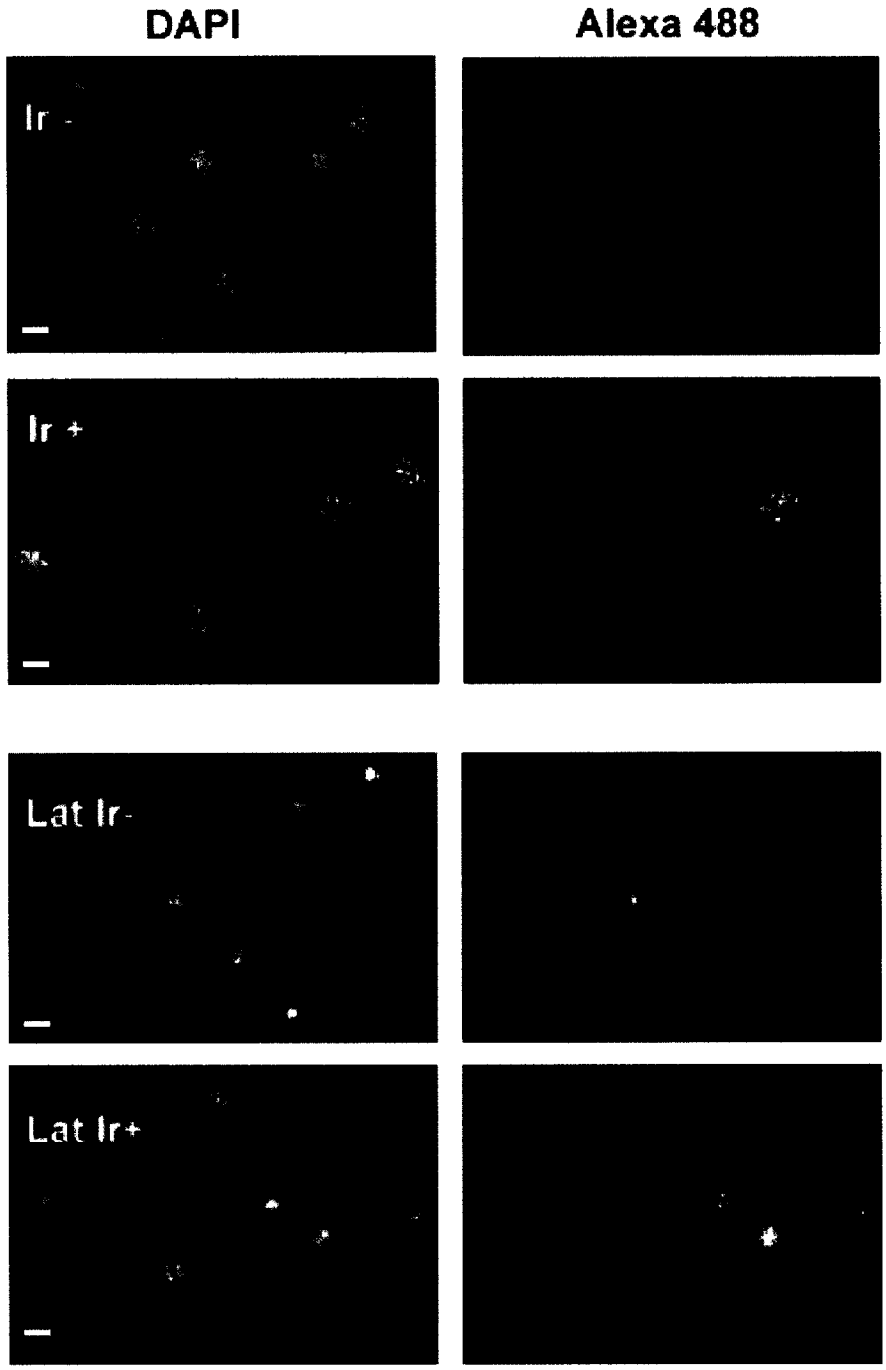

Figure 4-2. A difference in the amount of γ-H2AX in drug treated versus control cells is difficult to detect by visual inspection alone since latrunculin treatments cause shape changes. The left panel shows nuclei of 10T1/2 cells stained with DAPI and the right panel shows the corresponding γ-H2AX signal shown by Alexa 488 secondary antibody. The top group of images are non-drug treated cells with and without irradiation, whereas the bottom images are latrunculin B treated cells with and without irradiation. A 20X dry fluar lens (numerical aperture = 0.75) was used to obtain images. The scale bars represent 10 μm.

Although the overlapping signal appears brighter the size of the cell has to be considered. The same is seen when comparing the DAPI images of control and latrunculin treated cells. Although the latrunculin treated cells appear brighter, two-dimensional analysis determines that they actually have a significantly diminished γ-H2AX signal in comparison to non-treated cells. Since the analysis considers the total intensity of the signal regardless of the cell size it should be a reliable measurement. However, the rounding of the cells caused by latrunculin treatments creates differences between the non-treated and latrunculin treated cells in the Z-axis. Since the collection and analysis of the images is two-dimensional it is difficult to be sure that the differences in the cells Z plane are being measured. The use of a lens with a lower numerical aperture captures light from the entire Z plane and therefore corrects for this problem. However, an additional way to correct for shape change is to normalize the total intensity from the Alexa 488 channel to the total intensity of the DAPI signal. This also corrects for variable amounts of DNA and therefore variable amounts of histones confounding the amount of γ-H2AX signal. Although the scale of the intensity changes the overall pattern of change remains nearly the same. If there is a difference, it is likely that the total intensity measurements are an underestimation of actual differences (Table 4-2).

	Comparing	H2AX intensities	Ratio
Total Intensity of γ-H2AX	Ir+ / Ir-	$1.484 \times 10^6 / 0.389 \times 10^6$	3.81
	Ir+ / Lat Ir+	$1.484 \times 10^6 / 0.8269 \times 10^6$	1.79
	Ir- / Lat Ir-	$0.389 \times 10^6 / 0.284 \times 10^6$	1.37
	Lat Ir+ / Lat Ir-	$0.827 \times 10^6 / 0.284 \times 10^6$	2.91
Normalized Intensity of γ-H2AX	Ir+ / Ir-	1.125 / 0.2571	4.38
	Ir+ / Lat Ir+	1.125 / 0.6597	1.71
	Ir- / Lat Ir-	0.2571 / 0.1781	1.44
	Lat Ir+ / Lat Ir-	0.6597 / 0.1781	3.70

Table 4-2. Data on the total intensity of γ-H2AX and the intensity of γ-H2AX normalized to the amount of DNA shows similar decreases in response to latrunculin B treatments. All treatments are in 10T1/2 cells.

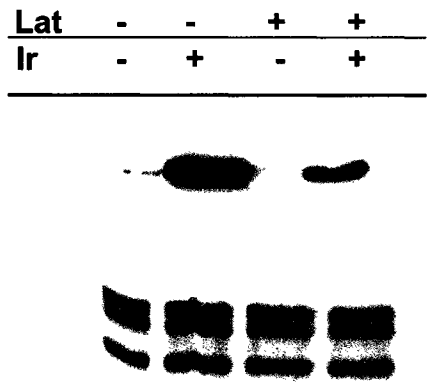

Figure 4-3. Disruption of F-actin causes a decrease in H2AX γ-phosphorylation in response to irradiation as seen by western blotting. A coomassie gel ran in parallel confirms equal loading. The result shown is representative of multiple experimental replicates.

Immunoblot analysis confirmed the data from immunofluorescence microscopy and Metamorph analysis. Parallel coomassie gels were used as loading controls (Figure 4-3). Blots were also stained with copper (II) phthalocyanine 3,4,4'',4''' tetrasulfonic acid tetrasodium salt (CPTS) as an internal loading control. The result confirms a decrease in γ-H2AX in latrunculin treated irradiated cells. Latrunculin treated non-irradiated cells also appear to have a lower basal level of γ-H2AX.

Flow cytometry was also used to confirm the finding that latrunculin treatments result in decreased levels of γ-H2AX (Figure 4-4). The large numbers of cells used results in very small errors of the mean. In fact, in the non-irradiated cells the error is so small that the error bars are not visible on this scale. The irradiated cells have larger error bars since there is more variation in the levels of γ-H2AX within irradiated cells.

Figure 4-5 provides another way of visualizing the difference in γ-H2AX levels in non-drug treated irradiated cells in comparison to latrunculin B treated irradiated cells, as analyzed by flow cytometry. The x-axis represents the intensity of γ-H2AX and the y-axis is the number of cell counts. The latrunculin treated cells clearly have less γ-H2AX intensity (as seen by the leftward shift in intensity) in comparison to the control irradiated cells. Once again the ratios of difference are similar to those of total intensity and normalized intensity from data collected by microscopy (Table 4-3).

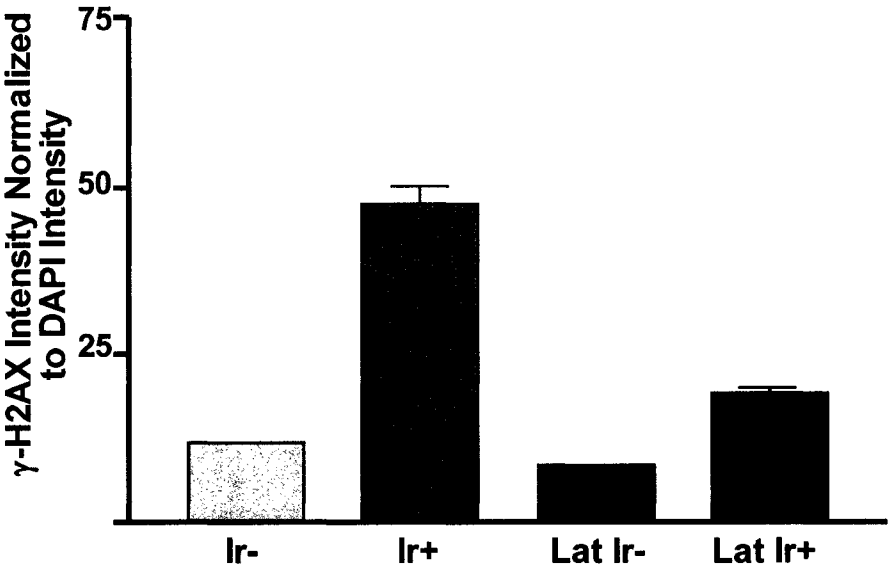

Figure 4-4. Disruption of F-actin causes a decrease in γ-H2AX as shown by flow cytometry. 10T1/2 cells received drug treatments of 20 μM latrunculin and irradiation of 5 Gy. A representative result is shown. Experiment was performed in triplicate.

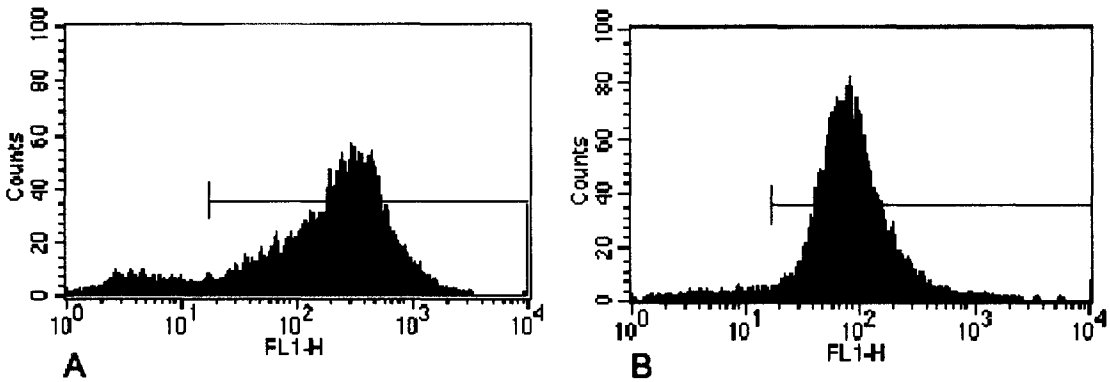

Figure 4-5. Disruption of F-actin causes a large decrease in γ-H2AX in irradiated cells. A) Represents non-drug treated irradiated 10T1/2 cells. B) Represents 20 μM latrunculin B treated irradiated 10T1/2 cells. The shift to the left in B) indicates a decrease in H2AX γ-phosphorylation. A representative result is shown. Experiment was performed in triplicate.

	Comparing	H2AX intensities	Ratio
Normalized Intensity of γ-H2AX	Ir+ / Ir-	47.73 / 11.92	4.00
	Ir+ / Lat Ir+	47.73 / 19.73	2.42
	Ir- / Lat Ir-	11.92 / 8.50	1.40
	Lat Ir+ / Lat Ir-	19.73 / 8.50	2.32

Table 4-3. Comparisons of irradiated and drug treated cells analyzed by flow cytometry. The ratios shown are consistent with previous findings of total intensity and normalized intensity measurements from immunofluorescence microscopy images.

Section 4.3. Disruption of filamentous actin affects γ-H2AX in ATM deficient cells

Section 4.3.1. γ-H2AX levels in wortmannin and latrunculin B treated cells

H2AX phosphorylation is thought to be achieved by one or all of the PIKK-kinases ATM, DNA-PK, or ATR (ATM and Rad3-related) with early studies implicating DNA-PK as the likely kinase [155]. However in 2001, using cell lines lacking the catalytic subunit of DNA-PK, Burma *et al.* found that H2AX focus formation remained normal despite the DNA-PK deficiency [153]. Instead, cell lines without functional ATM were severely compromised in γ-H2AX foci formation and the remaining levels of γ-H2AX were eliminated by low doses of wortmannin, which abolish the function of DNA-PK but not ATR [153]. Taken together, these results implicate ATM as the kinase primarily responsible for H2AX phosphorylation and that DNA-PK is responsible for a small amount of phosphorylation.

Wortmannin, a drug that inhibits PIKK kinases, was used as a control for the inhibition of H2AX phosphorylation. At lower concentrations, only ATM and DNA-PK are inhibited. Concentrations of about 5 μM result in half-maximal inhibition of ATM and DNA-PK whereas; ATR is more resistant to this drug with half-maximal inhibition at concentrations higher than 100 μM [162]. The use of 20 μM wortmannin resulted in significant reductions in γ-phosphorylation of H2AX in response to irradiation (Figure 4-6).

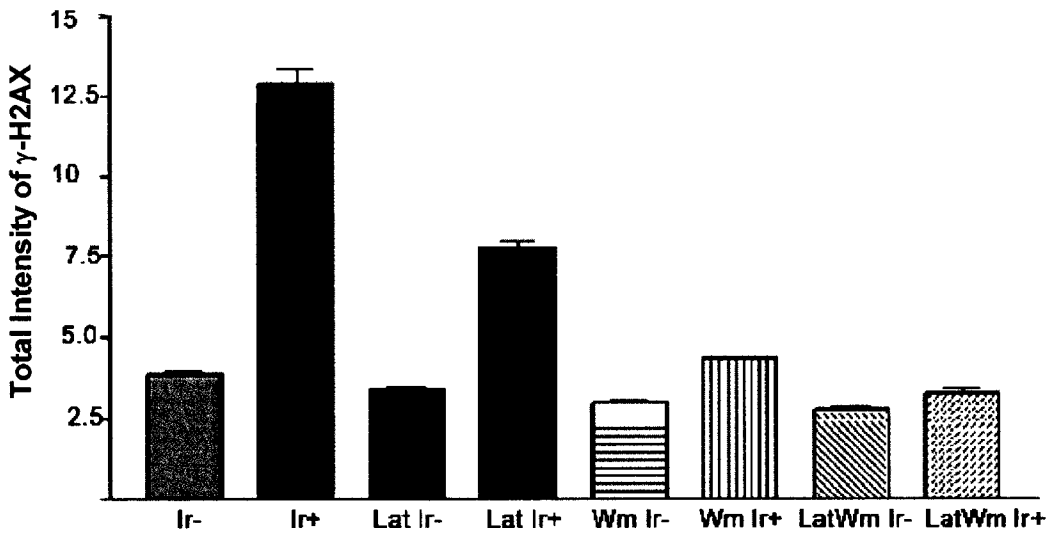

Figure 4-6. Disruption of F-actin in combination with the inhibition of PIKK kinases nearly eliminates H2AX γ-phosphorylation. 10T1/2 cells received drug treatments of either 20 μM latrunculin B, 20 μM wortmannin, or the drug treatments combined. Irradiation was 5 Gy. The result shown is representative of multiple experimental replicates.

Non-drug treated irradiated cells had almost three times more γ-H2AX than wortmannin treated irradiated cells. Latrunculin treated irradiated cells had almost double the amount of γ-H2AX in comparison to wortmannin treated irradiated cells. When wortmannin and latrunculin drug treatments were combined, the response to irradiation was nearly eliminated. Thus, the disruption of F-actin may decrease γ-phosphorylation of H2AX through the inhibition of ATM or DNA-PK, or through some other mechanism such as mediating phosphatase activity.

Section 4.3.2. γ-H2AX levels in cells lacking functional ATM kinase

Cell lines derived from patients with the disease ataxia telangiectasia are defective in ATM kinase. AT2BE is one such cell line. AT2BE cells were used to study the effects of F-actin disruption in the absence of ATM on H2AX γ-phosphorylation. If the disruption of F-actin does not result in a change in γ-H2AX levels in these cells, it would indicate that the changes seen in previous experiments were due to disruption at the level of the ATM kinase. To test this idea, AT2BE cells received latrunculin B treatments followed by irradiation, incubation, fixation, and staining with immunofluorescence antibodies. Quantification of images obtained by fluorescence microscopy reveal a pattern of response similar to the 10T1/2 cells that have functional ATM (Figure 4-7). Although the levels of phosphorylation are low due to the lack of ATM the response to latrunculin B is the same. These results suggest a role for F-actin in H2AX γ-phosphorylation at a point independent, but not necessarily exclusive, of phosphorylation by ATM kinase.

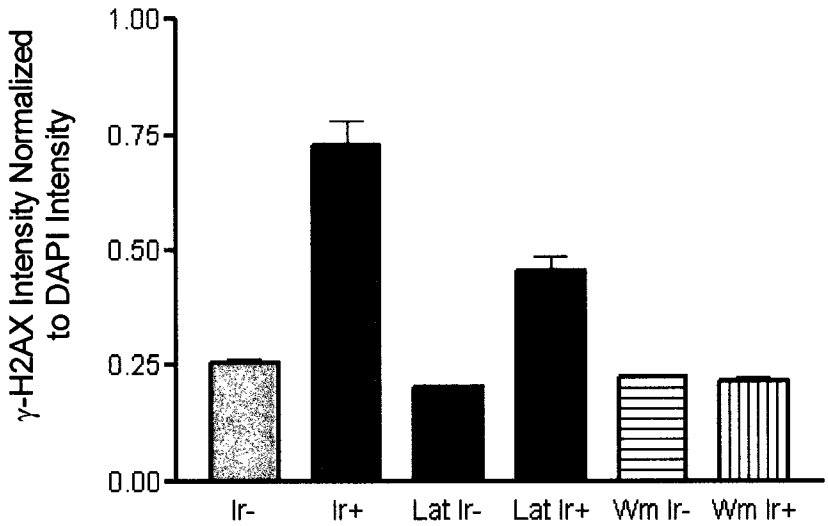

Figure 4-7. Disruption of F-actin and inhibition of PIKK kinases decrease the amount of γ-H2AX in ATM deficient cells. AT2BE cells received drug treatments of either 20 μM latrunculin B, or 20 μM wortmannin. Irradiation was 5 Gy. Data shown is representative of an experiment done in triplicate.

Section 4.4. Disruption of filamentous actin affects ATM activity

To investigate whether or not F-actin may have a role in ATM activation, HeLa and 10T1/2 cells were treated with 20 μM latrunculin B for 40 minutes or no drug treatment and with and without 5 Gy irradiation followed by fifteen minutes of post-irradiation incubation. The cells were then fixed and stained for the phosphorylated and activated form of ATM. Image acquisition and quantitative analysis using Metamorph software were carried out as before with the intensity of the Alexa 488 signal being representative of the activated ATM. Once again, the Alexa 488 image was normalized to the DAPI image to ensure more accurate measurements despite shape changes due to latrunculin treatments.

The latrunculin B treatments resulted in a decrease in phosphorylated ATM in both non-irradiated and irradiated cells in both 10T1/2 and HeLa cells (Figure 4-8 and 4-9). The large reduction in the levels of phosphorylated ATM in response to latrunculin B treatments suggests F-actin has a role in maintaining the basal levels of phosphorylated ATM. In the presence of latrunculin, ATM is still phosphorylated in response to irradiation however; this response is even less robust than the non-drug treated non-irradiated cells. Clearly, the disruption of F-actin has a large influence on the levels of ATM phosphorylation.

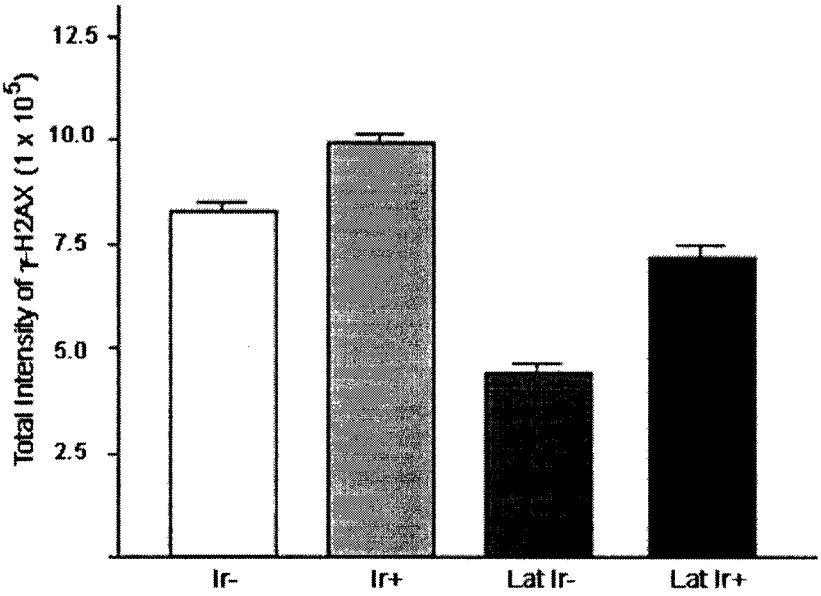

Figure 4-8. Disruption of F-actin decreases levels of phosphorylated ATM in 10T1/2 cells. Cells received drug treatments of 20 μM latrunculin B and irradiation of 5 Gy. Data shown is representative of an experiment done in triplicate.

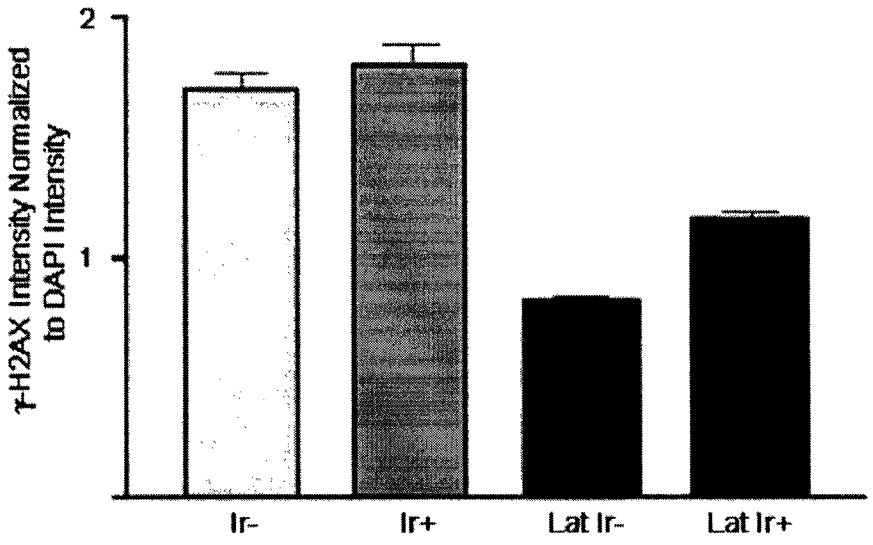

Figure 4-9. Disruption of F-actin decreases levels of phosphorylated ATM in HeLa cells. Cells received drug treatments of 20 μM latrunculin B and irradiation of 5 Gy. Data shown is representative of an experiment done in triplicate.

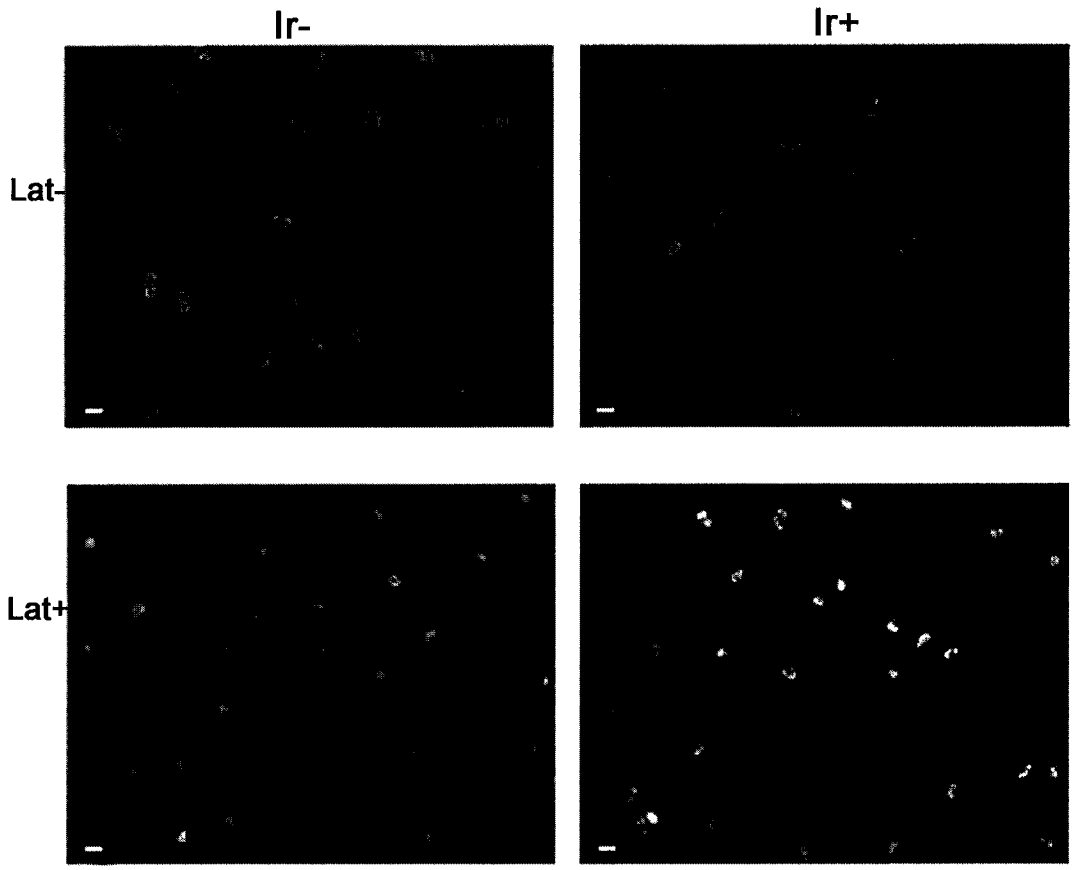

Figure 4-10. Changes in levels of phosphorylation of ATM kinase in cells with decreased F-actin in response to irradiation. All images are of the phosphorylated form of ATM as represented by an Alexa 488 stain. The two images on the left are of non-irradiated cells whereas the right images are of cells irradiated with 5Gy. The two upper panels are non-drug treated control HeLa cells and the two lower panels are 20 μM latrunculin B treated HeLa cells. A 20X dry fluar lens (numerical aperture = 0.75) was used to obtain images. The scale bars represent 10 μm.

Surprisingly, the increase in phospho-ATM levels in response to irradiation in non-drug treated control cells was small. In primary human fibroblasts, phosphorylation is normally detected immediately after exposure to 0.5 Gy irradiation, is maximal at 5 minutes, and remains stable for at least 24 hours [154]. Bakkenist *et al.* have characterized the specificity of the monoclonal antibody to ATM [154]. Peptide analysis as well as numerous immunoprecipitation experiments using constructs encoding various modifications to the ATM kinase demonstrated the specificity [154]. The lack of a large increase in phosphorylated ATM in response to irradiation in non-drug treated cells as seen in Figure 4-9 is thus unanticipated.

4.5. Chapter Summary

The induction of DNA double strand breaks is followed by the phosphorylation of serine 139 in the minor histone variant H2AX [148]. Members of the PIKK kinase family are responsible for the γ-phosphorylation of H2AX. In particular, ATM is the main kinase responsible for H2AX phosphorylation with DNA-PK being responsible for only small levels of phosphorylation [153]. ATM becomes activated through a process of autophosphorylation. This is thought to result from a general change in the nucleus, potentially in higher-order chromatin structure, rather than specific DNA breaks [154]. Since F-actin is believed to be a component of nuclear architecture it was hypothesized that the disruption of F-actin would cause nuclear structural changes that result in the autophosphorylation and activation of ATM, in turn increasing H2AX γ-phosphorylation. Instead, quantitative imaging

microscopy, western blotting, and flow cytometry show that the disruption of F-actin decreases γ-H2AX. A possible reason for this decrease is an inhibition of the kinase(s) responsible for γ-phosphorylation. In cells void of functional ATM a reduction in γ-H2AX in latrunculin treated cells is still seen indicating that F-actin may be involved in DNA-PK kinase activity, phosphatase activity, or some other pathway involved in H2AX γ-phosphorylation. The finding that the reduction in γ-H2AX levels in response to latrunculin treatments in ATM deficient cells is only ~30% whereas the reduction is ~60% in ATM competent cells suggests that F-actin disruption may inhibit the ATM kinase as well. This was investigated through the use of antibodies that detect the phosphorylated form of ATM. The finding that latrunculin treatments reduce the level of phosphorylated ATM in both non-irradiated and irradiated cells suggests that background levels of phosphorylated ATM are high in HeLa and 10T1/2 cells and that F-actin is necessary in maintaining these high levels. In addition, the small difference between the non-irradiated and irradiated cells under control conditions was unexpected. However, this small increase of ~5% may still be responsible for the increase observed in γ-H2AX levels in response to irradiation.

It is also possible that actin has a role in the functionality of phosphatases. Perhaps F-actin inhibits the activity of certain phosphatases and thus disruption of F-actin results in an increase in phosphatase activity and a subsequent reduction in γ-H2AX and phosphorylated ATM. The exact mechanism for elimination of γ-H2AX during DNA repair is largely unknown; however studies monitoring the redistribution of green fluorescent protein (GFP)- H2AX fusion constructs after photobleaching

have provided some insight [163]. Two mechanisms examined were, either phosphorylation and dephosphorylation of H2AX occurs in chromatin, or phosphorylation and dephosphorylation occurs in free H2AX that diffuses and exchanges with chromatin bound H2AX. When GFP-H2AX is transiently expressed it is found to have tight nuclear localization and is chromatin bound. After photobleaching areas of the nucleus, very little recovery of GFP-H2AX is observed, with an estimated mobile fraction of less than 20% [163]. Inflicting double-strand DNA breaks does not significantly increase the mobility of GFP-H2AX and, importantly, the mobility of GFP-H2AX does not change over a 60 minute time period when a 70% decrease in γ-H2AX is observed [148]. These results suggest that the formation and elimination of γ-H2AX in chromatin is unlikely to occur through diffusion and exchange with free histones. Instead, γ-H2AX is probably formed by phosphorylation at the sites of DNA breaks and likewise eliminated by dephosphorylation of the chromatin bound γ-H2AX [163].

An additional consideration is which phosphatase is responsible for dephosphorylating γ-H2AX. Protein phosphatase 1 (PP-1), which is the phosphatase responsible for the dephosphorylation of phosphorylated serine-10 histone H3, was found to dephosphorylate γ-H2AX *in vitro* [163]. The dephosphorylation of γ-H2AX by PP-1 is more efficient in the presence of the nuclear extract as opposed to just the purified H2AX [163]. This suggests that another nuclear factor may help to target PP-1 to H2AX. When calyculin A, a well-known inhibitor of PP-1 and protein phosphatase 2A (PP-2A), is used the elimination of γ-H2AX is inhibited as well as a partial inhibition of double strand break rejoining [164]. Unfortunately, it is not known

which mechanism this calyculin-sensitive phosphatase works through to result in γ-H2AX dephosphorylation. Some possibilities are that it is constitutively active and is either dominated by protein kinase activity at the site of the break or is transiently inactivated during double strand break repair and reactivated after repair. Another possibility is that the phosphatase is constitutively inactive and is transiently activated after break repair so to dephosphorylated γ-H2AX. In this case, F-actin could be necessary for maintaining the phosphatase in its inactive state and upon latrunculin treatments the phosphatase is activated and able to dephosphorylate γ-H2AX.

Chapter 5: Discussion

Section 5.1. Identifying Structural Proteins in the Nucleus

The study of the nuclear matrix has been a lengthy and difficult journey yet; the result has culminated in substantial evidence for the nuclear matrix as a genuine structure rather than a mere notion. The specific attachments of chromatin fibers to the nuclear matrix as well as the identification of a growing number of spatially distinct, functional nuclear domains implicate the matrix in mediating elaborate spatial organization. Conceptually, this allows for the involvement of the nuclear matrix in potentially all nuclear processes. Indeed, the body of pertinent research implicating the matrix in having functional associations with DNA attachment [165], DNA replication [166], RNA transcription [167], RNA splicing [168], and viral functions [169], is vast. Although studies on nuclear matrix function have been extensive, the characterization of the structural molecules in the matrix and their mechanisms of assembly have not been exhaustive. Matrix isolation by a variety of different procedures, including removing chromatin by electroelution, reveal the same underlying network of core filaments [170]. On the basis of these findings, it was proposed that the internal nuclear matrix is constructed on an underlying network of branched 10-nm filaments [170]. In this model other nuclear matrix components, including the ribonucleoprotein network, are positioned by direct and indirect attachments to the 10-nm filaments.

Section 5.1.1. Nuclear lamins

The characterization of the 10-nm core filament composition is still under debate. Many proteins have been proposed but, so far, the principal structural component of the filaments has not been determined. Lamins are the major proteins comprising the nuclear lamina, which forms the proteinaceous layer found at the interface between chromatin and the inner nuclear membrane [171]. These type V intermediate filament proteins are subdivided into A types, expressed in differentiated cells, and B types, found in all cells [172]. The central rod domain of the lamins consist of heptad repeats that drive the interaction between two lamin protein chains, to form a coiled-coil dimer, which is the basic structural unit of lamin assembly [173]. Cytoskeletal intermediate filament proteins assemble into 10-nm filaments both *in vitro* and *in situ*. However, similar filaments are rarely seen in studies of lamin assembly. Instead the final *in vitro* lamin assembly products are large paracrystalline arrays. These paracrystals do not exist *in vivo* under normal circumstances and are thought to result from lateral stacking of filamentous structures [173]. The marked difference between lamin assembly *in vivo* and *in vitro* suggests that lamin organization *in vivo* is regulated by interactions with other molecules. Furthermore, the inability of most lamins to assemble into 10-nm intermediate filaments may be related to the fact that they have six additional heptads in their central rod domain in comparison to cytoskeletal intermediate filament proteins [173].

In addition to the lamina, there is also evidence that the lamins form nucleoplasmic structures. Immunofluorescence and GFP-lamin live-cell imaging

show that these structures appear as either distinct foci or as a veil that fills the nucleoplasm [174,175]. The use of fluorescence recovery after photobleaching shows that these structures are not just pools of unincorporated, freely diffusing lamins but instead the fluorescence recovery rates suggest relatively stable structures [175]. Immunoelectron microscopy evidence detects lamins at sites along nuclear filaments [176]. However, the inability of lamins to form 10-nm filaments as well as the low level of staining suggests that lamins are not the major filamentous proteins of the nucleoplasm. Still, it is likely that proper nuclear function depends upon interactions and crosstalk between the nuclear matrix (regardless of its composition) and the lamina.

Section 5.1.2. Nuclear actin

Actin is a major protein identified in nuclear matrix protein preparations [22,177,178], and recent data suggests that it is in its filamentous form [27,179]. There are numerous actin-binding proteins in the nucleus, perhaps most notably, a myosin I isoform and structural protein 4.1 [41,137]. In the human red blood cell, protein 4.1 links spectrin-actin complexes to plasma membrane-associated proteins [41]. When *Xenopus* interphase extracts are depleted of the nuclear isoform of protein 4.1, nuclear assembly is inhibited [41]. Furthermore, actin and actin-related proteins (ARPs) have been found in chromatin remodeling complexes, which use energy from ATP hydrolysis to render nucleosomal DNA more accessible [126]. In the chromatin remodeling BAF complex, actin is tightly bound and removal results in the loss of

ATPase activity as well as the inability of the complex to associate with the nuclear matrix [126]. Taken together, these findings suggest actin has important roles in nuclear processes perhaps even as the all-encompassing primary core structural filament of the nuclear matrix.

Section 5.1.3. Additional candidates for core filaments in the nuclear matrix

Suggestions for nuclear core filaments have included the hnRNP proteins A2 and/or B1. After RNase digestion or salt extraction these proteins reassemble into helical filaments that are 7-18 nm in diameter and have a pitch of 60 nm [180]. However, the 10-nm core filaments of the nuclear matrix are not helical and, like intermediate filaments, have axial repeats of 23 nm [170]. This, along with the fact that antibodies recognizing hnRNP A2 and B1 do not stain core filaments[181], makes it unlikely that hnRNP A2 or hnRNP B1 are primary core structural filaments.

A significant development in the study of nuclear matrix proteins was the demonstration that NuMA (nuclear mitotic apparatus protein) is a nuclear matrix protein [182]. NuMA has an unusual pattern of segregation during mitosis. Upon nuclear envelope breakdown it associates with the spindle and progresses down the spindle microtubules to concentrate ultimately at the pericentrosomal region [183]. The ability of this large protein, which is over 200kDa, to form long coiled-coil structures suggested an important role for NuMA in the organization of the nuclear matrix [183]. However, it is unlikely that NuMA is the primary core filament since an antibody against NuMA labels only a ~15% subfraction of nuclear filaments [182]. On the other

hand, the finding that NuMA can self assemble into multi-arm oligomers both *in vitro* and after overexpression in cells suggests that it may be an important structural protein in nuclear architecture to some capacity [184,185].

Section 5.1.4. Potentials for crosstalk and interactions of skeletal networks

Many components of the cytoskeletal network have counterparts in the nucleoskeleton and some of these elements can connect intermediate filaments and coordinate skeletal networks. For example, plectin forms bridges from vimentin to actin filaments and recent evidence suggests plectin is present at the nuclear surface with specific binding to lamin B [186]. Other proteins that could serve to link skeletal components of the matrix are the novel nuclear proteins characterized by spectrin repeats (SRs), including Syne-1 and –2[187], Myne-1[188], Nesprin-1 and –2[189,190], and NUANCE[191]. These proteins have been identified as components of the nuclear envelope and their carboxy-terminal transmembrane domain is thought to anchor them to the nuclear membrane [190,191]. Antibodies against these SR proteins show an intense nuclear stain that is similar to lamin A patterns and these proteins immunoprecipitate with lamin A. Furthermore, the carboxy-terminus of Nesprin binds directly to lamin A lending additional support for SR proteins being nuclear membrane components [190,192]. The finding that SR proteins contain a calponin homology domain, known for binding actin, allows for the possibility that these proteins function in linking the inner nuclear membrane, the lamina, and nuclear actin [190,191]. Furthermore, the recent discovery of protein 4.1 in the nucleus suggests that it

could stabilize interactions of SR proteins with actin in much the same way that it links spectrin-actin complexes to plasma membrane proteins in the red cell membrane skeleton [42]. In fact, protein 4.1 can also bind to another nuclear structural protein candidate, NuMA, providing yet a further mechanism for linking various nuclear structures [193].

Section 5.2. Changes in transcription levels in response to disruption of F-actin

The potential mechanisms through which F-actin could exercise transcriptional control are vast. Most generally, if actin is a component of the nuclear matrix, it is likely that disruption of this network would result in a decrease in transcriptional activity. This is because the actual process of transcription is thought to happen at the nuclear matrix. It is proposed that transcription occurs when the chromatin fiber moves through a large multi-protein transcription complex bound to the matrix [95,194]. The transcriptionally inactive genes are in a condensed higher order chromatin structure whereas the active genes are in DNase sensitive regions that are decondensed and accessible to transcription machinery [64]. Matrix attachment regions (MARs), at the base of decondensed active chromatin loops, have been shown to bind nuclear matrix proteins and may anchor the necessary chromatin [101]. The components of the transcription machinery that are thought to mediate this interaction include some transcription factors and, enzymes such as histone acetyltransferases (HATs) and histone deacetylases (HDACs) [101]. The nuclear matrix is selective about which transcription factors it binds, varying by cell type and stages in differentiation and

development [101]. HATs and HDACs have also been shown to be abundant within the nuclear matrix [107]. The histones in transcriptionally active chromatin, which is closely associated with the matrix, have rapid cycles of acetylation followed by deacetylation [63] consequently; it is not surprising that the enzymes responsible for this change also have matrix associations. Having acetyltransferases at the matrix would allow for HATs and HDACs to mediate interactions between the transcriptionally active chromatin and the matrix [64]. To make a case for F-actin as a potential scaffold for this interaction, treatments with drugs that disrupt actin polymerization result in the release of a substantially larger amount of HATs and HDACs than previously released with traditional low-salt extraction procedures [120].

Actin may also mediate transcription through its role in chromatin remodeling complexes. The BAF complex, a mammalian homologue to yeast SWI/SNF, was the first complex to have actin identified as a component [126]. Subsequently, actin has been identified in multiple complexes from *Drosophila* to mammals [127,128]. Remodeling complexes work by altering nucleosome structure to allow for transcriptional machinery to access the DNA. The finding that BAF complexes that lack actin are unable to form associations with the nuclear matrix [126] suggests that actin could have important roles in regulating chromatin structure.

The importance of F-actin in transcriptional processes was confirmed through the use of latrunculin, a drug that inhibits actin polymerization resulting in the net depolymerization of actin. In the presence of this drug, immunofluorescence microscopy revealed that significantly less halogenated nucleoside was incorporated into newly synthesizing RNA. One potential problem is that changes to the

cytoskeleton could alter the structure of the nucleoskeleton through tensegrity. A tensegrity system is defined as an architectural construction that is comprised of an array of compression-resistant struts that do not touch one another but are interconnected by a continuous series of tension elements [195]. In this model, microtubules are considered the compression-resistant struts and actin microfilaments are tension elements due to their elastic and contractile properties. Tensegrity explains the coincident changes in nuclear structure with changes in the rest of the cell by mechanical coupling. For example, when a cell spreads, its nucleus extends in parallel even if some delay is seen in migrating cells [195]. This is also useful in explaining how extracellular mechanical stimuli can modify gene expression through deformation of the nucleus [195]. To counter the criticism that disrupting F-actin may be causing changes in nuclear processes through tensile changes in the cytoskeleton, suspension cells were compared with adherent cells using flow cytometry. Both the suspension cell line and the adherent line showed a decrease in transcriptional activity in response to F-actin depolymerization. These findings are consistent with nuclear F-actin having a role in transcription rather than general cellular shape changes causing decreases in transcriptional activity.

The change in levels of nuclear F-actin could decrease transcription through a variety of mechanisms. The decrease in polymerase I-transcription is most apparent by the almost complete elimination of nucleolar signal. It is thought that nucleolar architecture, which consists of, the fibrillar centers surrounded by the dense fibrillar components in turn surrounded by the granular components, is maintained by structural support provided by the nucleoskeleton [77]. After removing most of the

chromatin and dispersing the granular components and the dense fibrillar components, the fibrillar centers remained fixed to the nucleoskeleton [77]. Therefore, a possible theory for the reduction in RNA polymerase I mediated transcription is that the architecture of the nucleoli is altered in such a way that hinders function.

The disruption of RNA polymerase II transcription, as seen by the reduction in nucleoplasmic signal, could be due to the dismantling of an actin-based scaffold upon which transcription machinery assembles and functions. Likewise, the actin containing chromatin-remodeling complexes, which accumulate at sites of transcription on the matrix, could also be affected by the depolymerization of actin; however, the polymerization state of actin in these complexes is unknown. Another potential mechanism for functions of F-actin in transcriptional processes is through interactions with the recently identified nuclear myosin I isoform. This isoform has a unique amino-terminal extension that directs it to the nucleus where it is found to colocalize with RNA polymerase II [137]. When transcription is inhibited, the colocalization is also lost suggesting a transcription-dependent association [137]. The fact that myosin is an actin-based molecular motor raises the possibility that actin is also involved in transcription by RNA polymerase II. To lend credence to this theory, myosin light chain kinase inhibitors, which disrupt myosin-actin interactions also cause a decrease in the levels of transcription. These results provide a rationale for further investigation into the roles of actin, myosin, and their potential interaction in transcription. Additionally, investigating the necessity of F-actin in replication is also a worthwhile pursuit since replication shares many features with transcription in relation to the nuclear matrix. For example, there is substantial evidence that DNA

polymerases are immobilized upon a nuclear scaffold [96]. Furthermore, nuclear architecture that favors transcriptional seems to exert repression on replication and vice versa [121]. The fact that physical nuclear structures could coordinate and control both transcription and replication suggests that investigating replication in response to F-actin disruption could be useful.

Section 5.3. Changes in phosphorylation of H2AX and ATM kinase in response to disruption of F-actin

The histone variant H2AX is γ-phosphorylated at sites of DNA breaks [150]. In particular, the study of H2AX phosphorylation in response to double strand breaks caused by damage has been informative. γ-H2AX seems to have a role in the formation of repair foci as seen by the subsequent recruitment of numerous repair factors to the break sites [155]. In further support of a role for H2AX in repair, it was found that H2AX deficient mice have chromosomal instabilities, repair defects, and decreases in the recruitment of necessary proteins into repair foci [156]. There is evidence that repair occurs on the nuclear matrix and therefore it seems worthwhile to investigate the γ-phosphorylation of H2AX in the presence of drugs that disrupt F-actin. Some evidence for the involvement of the nuclear matrix in repair processes includes the finding that repair of cyclobutane dimers and/or (6-4) photoproducts takes place in association with the nuclear matrix [92,196], as well, repair enzymes such as poly(ADP-ribose) polymerase and DNA polymerase β are shown to preferentially localize on the matrix [197,198]. There is also evidence that more repair occurs at the

matrix than in the rest of the nucleoplasm, as seen by the repair of carcinogenic chromium-induced lesions; however, it is not clear whether or not these findings reflect the preferential repair of active genes over inactive genes [199]. Perhaps the more appealing motive for studying the potential role of F-actin in H2AX phosphorylation is that of the activation of ATM kinase. ATM is a phosphatidylinositol 3-kinase protein kinase-like (PIKK) and has been identified as the kinase primarily responsible for H2AX γ-phosphorylation in response to DNA double strand breaks [153]. The potentially interesting connection between F-actin and ATM is that ATM activation is thought to respond to changes in chromatin structure rather than DNA breaks *per se*. Even when cells receive very low exposure to ionizing irradiation (0.5 Gy), inflicting an estimated 18 DNA breaks, well over 50% of the total ATM is autophosphorylated [154]. It seems practical that the disruption of an F-actin scaffold could cause the inactive ATM, associated in dimers, to have a conformational change resulting in intermolecular autophosphorylation and activation.

When cells were treated with drugs that inhibit actin polymerization it was found that the levels of γ-H2AX decrease in both non-irradiated cells and irradiated cells. This was confirmed through quantitative immunofluorescence microscopy, western blotting, and flow cytometry. The mechanism for this reduction in γ-H2AX could be the result of a number of mechanisms involving either the initial phosphorylation by kinases, or the subsequent dephosphorylation by yet unidentified phosphatase(s). The reduction in γ-H2AX levels caused by actin depolymerization is not as severe as the reduction caused by inhibiting the PIKK kinases directly with the

drug wortmannin or as the reduction seen in cells lacking functional ATM. Still, F-actin disruption does cause a reduction in the amount of γ-H2AX. From this it is clear that F-actin has a role in either H2AX γ-phosphorylation or maintaining γ-H2AX levels that is independent, but not necessarily mutually exclusive of, the ATM kinase. Antibodies to phospho-ATM were used to reveal that disrupting F-actin does inhibit ATM phosphorylation. Interestingly, the phosphorylation of ATM in response to 5 Gy is minimal in both 10T1/2 and HeLa cells; however, it is still possible that these small changes in ATM phosphorylation cause large changes in H2AX phosphorylation. Furthermore, the disruption of F-actin could be inhibiting the activity of the DNA-PK kinase or inhibiting some other point in the process of H2AX phosphorylation. An alternative consideration to kinase activity is that F-actin may normally inhibit phosphatase activity and the depolymerization of actin releases this inhibition allowing the phosphatase to dephosphorylated ATM and/or H2AX.

A general criticism on this body of work is that although the aim is to study the effects of F-actin disruption on nuclear processes, the inhibition of F-actin is not specific to the nuclear actin pool. In the future, studies could be strengthened through the use of techniques that specifically target the depolymerization of nuclear F-actin. For example, there are multiple actin depolymerizing agents that could be carefully microinjected into the nucleus; likewise, the use of siRNA technology and mutant actins could result in the specific decrease in nuclear F-actin levels. For the time being, the findings that transcription and ATM/H2AX phosphorylation are inhibited in response to the disruption of cellular actin provides a basis for future investigation into the involvement of F-actin in these processes.

Bibliography

1. Straub, F.B. Actin. *Stud. Szeged* **2**, 3-15 (1942).

2. Kron, S.J., Drubin, D.G., Botstein, D. & Spudich, J.A. Yeast actin filaments display ATP-dependent sliding movement over surfaces coated with rabbit muscle myosin. *Proc Natl Acad Sci U S A* **89**, 4466-70 (1992).

3. Zechel, K. & Weber, K. Actins from mammals, bird, fish and slime mold characterized by isoelectric focusing in polyacrylamide gels. *Eur J Biochem* **89**, 105-12 (1978).

4. Sheterline, P., Clayton, J. & Sparrow, J. Actin. *Protein Profile* **2**, 1-103 (1995).

5. Vandekerckhove, J. & Weber, K. At least six different actins are expressed in a higher mammal: an analysis based on the amino acid sequence of the amino-terminal tryptic peptide. *J Mol Biol* **126**, 783-802 (1978).

6. Vandekerckhove, J., Franke, W.W. & Weber, K. Diversity of expression of non-muscle actin in amphibia. *J Mol Biol* **152**, 413-26 (1981).

7. Alberts, B., Bray, D., Lewis, J., Raff, M., Roberts, K., and Watson, J. *Molecular Biology of the Cell 3rd ed.*, (Garland Publishing Inc., 1994).

8. Wegner, A. & Engel, J. Kinetics of the cooperative association of actin to actin filaments. *Biophys Chem* **3**, 215-25 (1975).

9. Lodish, H., Berk, A., Zipursky, S., Matsudaira, P., Baltimore, D., and Darnell, J. *Molecular Cell Biology 4th ed.*, (W.H. Freeman and Company, 2000).

10. Wegner, A. & Isenberg, G. 12-fold difference between the critical monomer concentrations of the two ends of actin filaments in physiological salt conditions. *Proc Natl Acad Sci U S A* **80**, 4922-5 (1983).

11. Wegner, A. Head to tail polymerization of actin. *J Mol Biol* **108**, 139-50 (1976).

12. Jockusch, B.M., Becker, M., Hindennach, I. & Jockusch, E. Slime mould actin: homology to vertebrate actin and presence in the nucleus. *Exp Cell Res* **89**, 241-6 (1974).

13. Douvas, A.S., Harrington, C.A. & Bonner, J. Major nonhistone proteins of rat liver chromatin: preliminary identification of myosin, actin, tubulin, and tropomyosin. *Proc Natl Acad Sci U S A* **72**, 3902-6 (1975).

14. Lestourgeon, W.M., Forer, A., Yang, Y.Z., Bertram, J.S. & Pusch, H.P. Contractile proteins. Major components of nuclear and chromosome non-histone proteins. *Biochim Biophys Acta* **379**, 529-52 (1975).

15. Clark, T.G. & Merriam, R.W. Diffusible and bound actin nuclei of Xenopus laevis oocytes. *Cell* **12**, 883-91 (1977).

16. Rando, O.J., Zhao, K. & Crabtree, G.R. Searching for a function for nuclear actin. *Trends Cell Biol* **10**, 92-7 (2000).

17. Fukui, Y. Intranuclear actin bundles induced by dimethyl sulfoxide in interphase nucleus of Dictyostelium. *J Cell Biol* **76**, 146-57 (1978).

18. Clark, T.G. & Rosenbaum, J.L. An actin filament matrix in hand-isolated nuclei of X. laevis oocytes. *Cell* **18**, 1101-8 (1979).

19. Fukui, Y. & Katsumaru, H. Nuclear actin bundles in Amoeba, Dictyostelium and human HeLa cells induced by dimethyl sulfoxide. *Exp Cell Res* **120**, 451-5 (1979).

20. Osborn, M. & Weber, K. Dimethylsulfoxide and the ionophore A23187 affect the arrangement of actin and induce nuclear actin paracrystals in PtK2 cells. *Exp Cell Res* **129**, 103-14 (1980).

21. Gounon, P. & Karsenti, E. Involvement of contractile proteins in the changes in consistency of oocyte nucleoplasm of the newt Pleurodeles waltlii. *J Cell Biol* **88**, 410-21 (1981).

22. Nakayasu, H. & Ueda, K. Association of actin with the nuclear matrix from bovine lymphocytes. *Exp Cell Res* **143**, 55-62 (1983).

23. Welch, W.J. & Suhan, J.P. Morphological study of the mammalian stress response: characterization of changes in cytoplasmic organelles, cytoskeleton, and nucleoli, and appearance of intranuclear actin filaments in rat fibroblasts after heat-shock treatment. *J Cell Biol* **101**, 1198-211 (1985).

24. Parfenov, V.N. & Galaktionov, K.I. [Intranuclear actin microfilaments in the oocytes of the common frog]. *Tsitologiia* **29**, 142-9 (1987).

25. Lachapelle, M. & Aldrich, H.C. Phalloidin-gold complexes: a new tool for ultrastructural localization of F-actin. *J Histochem Cytochem* **36**, 1197-202 (1988).

26. Wada, A., Fukuda, M., Mishima, M. & Nishida, E. Nuclear export of actin: a novel mechanism regulating the subcellular localization of a major cytoskeletal protein. *Embo J* **17**, 1635-41 (1998).

27. McDonald, D., Carrero, G., Crawford, E., Andrin, C., de Vries, G., and Hendzel, M. Nuclear Beta Actin Exists in a Dynamic Equilibrium between Filaments and Monomers in Living Mammalian Cells. *Manuscript in preparation* (2004).

28. dos Remedios, C.G. et al. Actin binding proteins: regulation of cytoskeletal microfilaments. *Physiol Rev* **83**, 433-73 (2003).

29. Van Etten, R.A. et al. The COOH terminus of the c-Abl tyrosine kinase contains distinct F- and G-actin binding domains with bundling activity. *J Cell Biol* **124**, 325-40 (1994).

30. Weins, A. et al. Differentiation- and stress-dependent nuclear cytoplasmic redistribution of myopodin, a novel actin-bundling protein. *J Cell Biol* **155**, 393-404 (2001).

31. Iida, K., Iida, H. & Yahara, I. Heat shock induction of intranuclear actin rods in cultured mammalian cells. *Exp Cell Res* **165**, 207-15 (1986).

32. Prendergast, G.C. & Ziff, E.B. Mbh 1: a novel gelsolin/severin-related protein which binds actin in vitro and exhibits nuclear localization in vivo. *Embo J* **10**, 757-66 (1991).

33. Onoda, K. & Yin, H.L. gCap39 is phosphorylated. Stimulation by okadaic acid and preferential association with nuclei. *J Biol Chem* **268**, 4106-12 (1993).

34. Nebl, G., Meuer, S.C. & Samstag, Y. Dephosphorylation of serine 3 regulates nuclear translocation of cofilin. *J Biol Chem* **271**, 26276-80 (1996).

35. Yang, N. et al. Cofilin phosphorylation by LIM-kinase 1 and its role in Rac-mediated actin reorganization. *Nature* **393**, 809-12 (1998).

36. Iida, K., Matsumoto, S. & Yahara, I. The KKRKK sequence is involved in heat shock-induced nuclear translocation of the 18-kDa actin-binding protein, cofilin. *Cell Struct Funct* **17**, 39-46 (1992).

37. Abe, H., Nagaoka, R. & Obinata, T. Cytoplasmic localization and nuclear transport of cofilin in cultured myotubes. *Exp Cell Res* **206**, 1-10 (1993).

38. Samstag, Y. et al. Costimulatory signals for human T-cell activation induce nuclear translocation of pp19/cofilin. *Proc Natl Acad Sci U S A* **91**, 4494-8 (1994).

39. Sotiropoulos, A., Gineitis, D., Copeland, J. & Treisman, R. Signal-regulated activation of serum response factor is mediated by changes in actin dynamics. *Cell* **98**, 159-69 (1999).

40. Posern, G., Sotiropoulos, A. & Treisman, R. Mutant actins demonstrate a role for unpolymerized actin in control of transcription by serum response factor. *Mol Biol Cell* **13**, 4167-78 (2002).

41. Krauss, S.W. et al. Two distinct domains of protein 4.1 critical for assembly of functional nuclei in vitro. *J Biol Chem* **277**, 44339-46 (2002).

42. Krauss, S.W., Chen, C., Penman, S. & Heald, R. Nuclear actin and protein 4.1: essential interactions during nuclear assembly in vitro. *Proc Natl Acad Sci U S A* **100**, 10752-7 (2003).

43. Berezney, R. & Coffey, D.S. Identification of a nuclear protein matrix. *Biochem Biophys Res Commun* **60**, 1410-7 (1974).

44. Capco, D.G., Wan, K.M. & Penman, S. The nuclear matrix: three-dimensional architecture and protein composition. *Cell* **29**, 847-58 (1982).

45. Jackson, D.A. & Cook, P.R. A general method for preparing chromatin containing intact DNA. *Embo J* **4**, 913-8 (1985).

46. Cremer, T. et al. Rabl's model of the interphase chromosome arrangement tested in Chinese hamster cells by premature chromosome condensation and laser-UV-microbeam experiments. *Hum Genet* **60**, 46-56 (1982).

47. Abney, J.R., Cutler, B., Fillbach, M.L., Axelrod, D. & Scalettar, B.A. Chromatin dynamics in interphase nuclei and its implications for nuclear structure. *J Cell Biol* **137**, 1459-68 (1997).

48. Marshall, W.F. et al. Interphase chromosomes undergo constrained diffusional motion in living cells. *Curr Biol* **7**, 930-9 (1997).

49. Lewis, J.D. & Tollervey, D. Like attracts like: getting RNA processing together in the nucleus. *Science* **288**, 1385-9 (2000).

50. Misteli, T. Cell biology of transcription and pre-mRNA splicing: nuclear architecture meets nuclear function. *J Cell Sci* **113 (Pt 11)**, 1841-9 (2000).

51. Gall, J.G. Cajal bodies: the first 100 years. *Annu Rev Cell Dev Biol* **16**, 273-300 (2000).

52. Zhong, S., Salomoni, P. & Pandolfi, P.P. The transcriptional role of PML and the nuclear body. *Nat Cell Biol* **2**, E85-90 (2000).

53. Spector, D.L. Macromolecular domains within the cell nucleus. *Annu Rev Cell Biol* **9**, 265-315 (1993).

54. Kruhlak, M.J. et al. Reduced mobility of the alternate splicing factor (ASF) through the nucleoplasm and steady state speckle compartments. *J Cell Biol* **150**, 41-51 (2000).

55. Phair, R.D. & Misteli, T. High mobility of proteins in the mammalian cell nucleus. *Nature* **404**, 604-9 (2000).

56. Hendzel, M. Comparmentalization of the interchromatin space is mediated by obstructed diffusion. *Manuscript in preparation* (2004).

57. Steele, W.J. & Busch, H. Studies on the ribonucleic acid components of the nuclear ribonucleoprotein network. *Biochim Biophys Acta* **129**, 54-67 (1966).

58. Hendzel, M.J., Boisvert, F. & Bazett-Jones, D.P. Direct visualization of a protein nuclear architecture. *Mol Biol Cell* **10**, 2051-62 (1999).

59. Peters, K.E., Okada, T.A. & Comings, D.E. Chinese hamster nuclear proteins. An electrophoretic analysis of interphase, metaphase and nuclear matrix preparations. *Eur J Biochem* **129**, 221-32 (1982).

60. Verheijen, R., Kuijpers, H., Vooijs, P., van Venrooij, W. & Ramaekers, F. Protein composition of nuclear matrix preparations from HeLa cells: an immunochemical approach. *J Cell Sci* **80**, 103-22 (1986).

61. Gerdes, M.G., Carter, K.C., Moen, P.T., Jr. & Lawrence, J.B. Dynamic changes in the higher-level chromatin organization of specific sequences revealed by in situ hybridization to nuclear halos. *J Cell Biol* **126**, 289-304 (1994).

62. Andreeva, M., Markova, D., Loidl, P. & Djondjurov, L. Intranuclear compartmentalization of transcribed and nontranscribed c-myc sequences in Namalva-S cells. *Eur J Biochem* **207**, 887-94 (1992).

63. Hendzel, M.J., Delcuve, G.P. & Davie, J.R. Histone deacetylase is a component of the internal nuclear matrix. *J Biol Chem* **266**, 21936-42 (1991).

64. Davie, J.R. The nuclear matrix and the regulation of chromatin organization and function. *Int Rev Cytol* **162A**, 191-250 (1995).

65. Jackson, D.A. Chromatin domains and nuclear compartments: establishing sites of gene expression in eukaryotic nuclei. *Mol Biol Rep* **24**, 209-20 (1997).

66. Shaffer, C.D., Wallrath, L.L. & Elgin, S.C. Regulating genes by packaging domains: bits of heterochromatin in euchromatin? *Trends Genet* **9**, 35-7 (1993).

67. Tartof, K.D., Hobbs, C. & Jones, M. A structural basis for variegating position effects. *Cell* **37**, 869-78 (1984).

68. Strouboulis, J. & Wolffe, A.P. Functional compartmentalization of the nucleus. *J Cell Sci* **109 (Pt 8)**, 1991-2000 (1996).

69. Wansink, D.G., Sibon, O.C., Cremers, F.F., van Driel, R. & de Jong, L. Ultrastructural localization of active genes in nuclei of A431 cells. *J Cell Biochem* **62**, 10-8 (1996).

70. Zirbel, R.M., Mathieu, U.R., Kurz, A., Cremer, T. & Lichter, P. Evidence for a nuclear compartment of transcription and splicing located at chromosome domain boundaries. *Chromosome Res* **1**, 93-106 (1993).

71. Clemson, C.M. & Lawrence, J.B. Multifunctional compartments in the nucleus: insights from DNA and RNA localization. *J Cell Biochem* **62**, 181-90 (1996).

72. Fu, X.D. & Maniatis, T. Factor required for mammalian spliceosome assembly is localized to discrete regions in the nucleus. *Nature* **343**, 437-41 (1990).

73. Wang, J., Cao, L.G., Wang, Y.L. & Pederson, T. Localization of pre-messenger RNA at discrete nuclear sites. *Proc Natl Acad Sci U S A* **88**, 7391-5 (1991).

74. Carter, K.C., Taneja, K.L. & Lawrence, J.B. Discrete nuclear domains of poly(A) RNA and their relationship to the functional organization of the nucleus. *J Cell Biol* **115**, 1191-202 (1991).

75. Hendzel, M.J., Kruhlak, M.J. & Bazett-Jones, D.P. Organization of highly acetylated chromatin around sites of heterogeneous nuclear RNA accumulation. *Mol Biol Cell* **9**, 2491-507 (1998).

76. Scheer, U. & Benavente, R. Functional and dynamic aspects of the mammalian nucleolus. *Bioessays* **12**, 14-21 (1990).

77. Hozak, P., Cook, P.R., Schofer, C., Mosgoller, W. & Wachtler, F. Site of transcription of ribosomal RNA and intranucleolar structure in HeLa cells. *J Cell Sci* **107 (Pt 2)**, 639-48 (1994).

78. Scheer, U. & Rose, K.M. Localization of RNA polymerase I in interphase cells and mitotic chromosomes by light and electron microscopic immunocytochemistry. *Proc Natl Acad Sci U S A* **81**, 1431-5 (1984).

79. Raska, I., Reimer, G., Jarnik, M., Kostrouch, Z. & Raska, K., Jr. Does the synthesis of ribosomal RNA take place within nucleolar fibrillar centers or dense fibrillar components? *Biol Cell* **65**, 79-82 (1989).

80. Rendon, M.C. et al. Characterization and immunolocalization of a nucleolar antigen with anti-NOR serum in HeLa cells. *Exp Cell Res* **200**, 393-403 (1992).

81. Thiry, M. Ultrastructural detection of DNA within the nucleolus by sensitive molecular immunocytochemistry. *Exp Cell Res* **200**, 135-44 (1992).

82. Thiry, M. New data concerning the functional organization of the mammalian cell nucleolus: detection of RNA and rRNA by in situ molecular immunocytochemistry. *Nucleic Acids Res* **20**, 6195-200 (1992).

83. Ochs, R.L., Lischwe, M.A., Spohn, W.H. & Busch, H. Fibrillarin: a new protein of the nucleolus identified by autoimmune sera. *Biol Cell* **54**, 123-33 (1985).

84. Kass, S., Tyc, K., Steitz, J.A. & Sollner-Webb, B. The U3 small nucleolar ribonucleoprotein functions in the first step of preribosomal RNA processing. *Cell* **60**, 897-908 (1990).

85. Puvion-Dutilleul, F., Bachellerie, J.P. & Puvion, E. Nucleolar organization of HeLa cells as studied by in situ hybridization. *Chromosoma* **100**, 395-409 (1991).

86. Jordan, E.G. & McGovern, J.H. The quantitative relationship of the fibrillar centres and other nucleolar components to changes in growth conditions, serum deprivation and low doses of actinomycin D in cultured diploid human fibroblasts (strain MRC-5). *J Cell Sci* **52**, 373-89 (1981).

87. Haaf, T., Hayman, D.L. & Schmid, M. Quantitative determination of rDNA transcription units in vertebrate cells. *Exp Cell Res* **193**, 78-86 (1991).

88. Cook, P.R. *Principles of Nuclear Structure and Function*, (Wiley-Liss, 2001).

89. Weipoltshammer, K., Schofer, C., Wachtler, F. & Hozak, P. The transcription unit of ribosomal genes is attached to the nuclear skeleton. *Exp Cell Res* **227**, 374-9 (1996).

90. Meier, U.T. & Blobel, G. Nopp140 shuttles on tracks between nucleolus and cytoplasm. *Cell* **70**, 127-38 (1992).

91. Cook, P.R. The organization of replication and transcription. *Science* **284**, 1790-5 (1999).

92. Harless, J. & Hewitt, R.R. Intranuclear localization of UV-induced DNA repair in human VA13 cells. *Mutat Res* **183**, 177-84 (1987).

93. Jackson, D.A., McCready, S.J. & Cook, P.R. RNA is synthesized at the nuclear cage. *Nature* **292**, 552-5 (1981).

94. Jackson, D.A., Hassan, A.B., Errington, R.J. & Cook, P.R. Visualization of focal sites of transcription within human nuclei. *Embo J* **12**, 1059-65 (1993).

95. Iborra, F.J., Pombo, A., Jackson, D.A. & Cook, P.R. Active RNA polymerases are localized within discrete transcription "factories' in human nuclei. *J Cell Sci* **109 (Pt 6)**, 1427-36 (1996).

96. Berezney, R. & Coffey, D.S. Nuclear protein matrix: association with newly synthesized DNA. *Science* **189**, 291-3 (1975).

97. Jackson, D.A. & Cook, P.R. Replication occurs at a nucleoskeleton. *Embo J* **5**, 1403-10 (1986).

98. Nakamura, H., Morita, T. & Sato, C. Structural organizations of replicon domains during DNA synthetic phase in the mammalian nucleus. *Exp Cell Res* **165**, 291-7 (1986).

99. Newport, J. & Yan, H. Organization of DNA into foci during replication. *Curr Opin Cell Biol* **8**, 365-8 (1996).

100. Hozak, P., Hassan, A.B., Jackson, D.A. & Cook, P.R. Visualization of replication factories attached to nucleoskeleton. *Cell* **73**, 361-73 (1993).

101. Davie, J.R. Nuclear matrix, dynamic histone acetylation and transcriptionally active chromatin. *Mol Biol Rep* **24**, 197-207 (1997).

102. van Wijnen, A.J. et al. Nuclear matrix association of multiple sequence-specific DNA binding activities related to SP-1, ATF, CCAAT, C/EBP, OCT-1, and AP-1. *Biochemistry* **32**, 8397-402 (1993).

103. Sun, J.M., Chen, H.Y. & Davie, J.R. Nuclear factor 1 is a component of the nuclear matrix. *J Cell Biochem* **55**, 252-63 (1994).

104. Sun, J.M., Chen, H.Y., Litchfield, D.W. & Davie, J.R. Developmental changes in transcription factors associated with the nuclear matrix of chicken erythrocytes. *J Cell Biochem* **62**, 454-66 (1996).

105. Hendzel, M.J., Sun, J.M., Chen, H.Y., Rattner, J.B. & Davie, J.R. Histone acetyltransferase is associated with the nuclear matrix. *J Biol Chem* **269**, 22894-901 (1994).

106. Li, W., Chen, H.Y. & Davie, J.R. Properties of chicken erythrocyte histone deacetylase associated with the nuclear matrix. *Biochem J* **314 (Pt 2)**, 631-7 (1996).

107. Hendzel, M.J. & Davie, J.R. Nuclear distribution of histone deacetylase: a marker enzyme for the internal nuclear matrix. *Biochim Biophys Acta* **1130**, 307-13 (1992).

108. Hebbes, T.R., Thorne, A.W. & Crane-Robinson, C. A direct link between core histone acetylation and transcriptionally active chromatin. *Embo J* **7**, 1395-402 (1988).

109. Hebbes, T.R., Thorne, A.W., Clayton, A.L. & Crane-Robinson, C. Histone acetylation and globin gene switching. *Nucleic Acids Res* **20**, 1017-22 (1992).

110. Ridsdale, J.A., Hendzel, M.J., Delcuve, G.P. & Davie, J.R. Histone acetylation alters the capacity of the H1 histones to condense transcriptionally active/competent chromatin. *J Biol Chem* **265**, 5150-6 (1990).

111. Perry, C.A. & Annunziato, A.T. Histone acetylation reduces H1-mediated nucleosome interactions during chromatin assembly. *Exp Cell Res* **196**, 337-45 (1991).

112. Perry, C.A., Dadd, C.A., Allis, C.D. & Annunziato, A.T. Analysis of nucleosome assembly and histone exchange using antibodies specific for acetylated H4. *Biochemistry* **32**, 13605-14 (1993).

113. Li, W., Nagaraja, S., Delcuve, G.P., Hendzel, M.J. & Davie, J.R. Effects of histone acetylation, ubiquitination and variants on nucleosome stability. *Biochem J* **296 (Pt 3)**, 737-44 (1993).

114. Lee, D.Y., Hayes, J.J., Pruss, D. & Wolffe, A.P. A positive role for histone acetylation in transcription factor access to nucleosomal DNA. *Cell* **72**, 73-84 (1993).

115. Turner, B.M. Decoding the nucleosome. *Cell* **75**, 5-8 (1993).

116. Zhang, D.E. & Nelson, D.A. Histone acetylation in chicken erythrocytes. Rates of acetylation and evidence that histones in both active and potentially active chromatin are rapidly modified. *Biochem J* **250**, 233-40 (1988).

117. Zhang, D.E. & Nelson, D.A. Histone acetylation in chicken erythrocytes. Rates of deacetylation in immature and mature red blood cells. *Biochem J* **250**, 241-5 (1988).

118. Boffa, L.C. et al. Factors affecting nucleosome structure in transcriptionally active chromatin. Histone acetylation, nascent RNA and inhibitors of RNA synthesis. *Eur J Biochem* **194**, 811-23 (1990).

119. Dignam, J.D., Lebovitz, R.M. & Roeder, R.G. Accurate transcription initiation by RNA polymerase II in a soluble extract from isolated mammalian nuclei. *Nucleic Acids Res* **11**, 1475-89 (1983).

120. Andrin, C., Hendzel, M. F-actin dependent insolubility of chromatin modifying components. *Journal of Biological Chemistry* **In Press**(2004).

121. Wansink, D.G. et al. RNA polymerase II transcription is concentrated outside replication domains throughout S-phase. *J Cell Sci* **107 (Pt 6)**, 1449-56 (1994).

122. Wei, X. et al. Segregation of transcription and replication sites into higher order domains. *Science* **281**, 1502-6 (1998).

123. Kornberg, R.D. & Lorch, Y. Twenty-five years of the nucleosome, fundamental particle of the eukaryote chromosome. *Cell* **98**, 285-94 (1999).

124. Wolffe, A.P., Khochbin, S. & Dimitrov, S. What do linker histones do in chromatin? *Bioessays* **19**, 249-55 (1997).

125. Sudarsanam, P. & Winston, F. The Swi/Snf family nucleosome-remodeling complexes and transcriptional control. *Trends Genet* **16**, 345-51 (2000).

126. Zhao, K. et al. Rapid and phosphoinositol-dependent binding of the SWI/SNF-like BAF complex to chromatin after T lymphocyte receptor signaling. *Cell* **95**, 625-36 (1998).

127. Papoulas, O. et al. The Drosophila trithorax group proteins BRM, ASH1 and ASH2 are subunits of distinct protein complexes. *Development* **125**, 3955-66 (1998).

128. Shen, X., Mizuguchi, G., Hamiche, A. & Wu, C. A chromatin remodelling complex involved in transcription and DNA processing. *Nature* **406**, 541-4 (2000).

129. Galarneau, L. et al. Multiple links between the NuA4 histone acetyltransferase complex and epigenetic control of transcription. *Mol Cell* **5**, 927-37 (2000).

130. Ikura, T. et al. Involvement of the TIP60 histone acetylase complex in DNA repair and apoptosis. *Cell* **102**, 463-73 (2000).

131. Fuchs, M. et al. The p400 complex is an essential E1A transformation target. *Cell* **106**, 297-307 (2001).

132. Boyle, S. et al. The spatial organization of human chromosomes within the nuclei of normal and emerin-mutant cells. *Hum Mol Genet* **10**, 211-9 (2001).

133. Croft, J.A. et al. Differences in the localization and morphology of chromosomes in the human nucleus. *J Cell Biol* **145**, 1119-31 (1999).

134. Zink, D., Bornfleth, H., Visser, A., Cremer, C. & Cremer, T. Organization of early and late replicating DNA in human chromosome territories. *Exp Cell Res* **247**, 176-88 (1999).

135. Maldonado, E., Drapkin, R. & Reinberg, D. Purification of human RNA polymerase II and general transcription factors. *Methods Enzymol* **274**, 72-100 (1996).

136. Bornfleth, H., Edelmann, P., Zink, D., Cremer, T. & Cremer, C. Quantitative motion analysis of subchromosomal foci in living cells using four-dimensional microscopy. *Biophys J* **77**, 2871-86 (1999).

137. Nowak, G. et al. Evidence for the presence of myosin I in the nucleus. *J Biol Chem* **272**, 17176-81 (1997).

138. Pestic-Dragovich, L. et al. A myosin I isoform in the nucleus. *Science* **290**, 337-41 (2000).

139. Saitoh, M., Ishikawa, T., Matsushima, S., Naka, M. & Hidaka, H. Selective inhibition of catalytic activity of smooth muscle myosin light chain kinase. *J Biol Chem* **262**, 7796-801 (1987).

140. Mabuchi, I., Takano-Ohmuro, H. Effects of inhibitors of myosin light chain kinase and other protein kinases on the first cell division of sea urchin eggs. *Dev Growth Differ* **32**, 549-556 (1990).

141. Higuchi, H. & Takemori, S. Butanedione monoxime suppresses contraction and ATPase activity of rabbit skeletal muscle. *J Biochem (Tokyo)* **105**, 638-43 (1989).

142. Scheer, U., Hinssen, H., Franke, W.W. & Jockusch, B.M. Microinjection of actin-binding proteins and actin antibodies demonstrates involvement of nuclear actin in transcription of lampbrush chromosomes. *Cell* **39**, 111-22 (1984).

143. Koleske, A.J. & Young, R.A. The RNA polymerase II holoenzyme and its implications for gene regulation. *Trends Biochem Sci* **20**, 113-6 (1995).

144. Ostap, E.M. 2,3-Butanedione monoxime (BDM) as a myosin inhibitor. *J Muscle Res Cell Motil* **23**, 305-8 (2002).

145. Kanaar, R., Hoeijmakers, J.H. & van Gent, D.C. Molecular mechanisms of DNA double strand break repair. *Trends Cell Biol* **8**, 483-9 (1998).

146. Rogakou, E.P., Boon, C., Redon, C. & Bonner, W.M. Megabase chromatin domains involved in DNA double-strand breaks in vivo. *J Cell Biol* **146**, 905-16 (1999).

147. Redon, C. et al. Histone H2A variants H2AX and H2AZ. *Curr Opin Genet Dev* **12**, 162-9 (2002).

148. Rogakou, E.P., Pilch, D.R., Orr, A.H., Ivanova, V.S. & Bonner, W.M. DNA double-stranded breaks induce histone H2AX phosphorylation on serine 139. *J Biol Chem* **273**, 5858-68 (1998).

149. Chen, H.T. et al. Response to RAG-mediated VDJ cleavage by NBS1 and gamma-H2AX. *Science* **290**, 1962-5 (2000).

150. Rogakou, E.P., Nieves-Neira, W., Boon, C., Pommier, Y. & Bonner, W.M. Initiation of DNA fragmentation during apoptosis induces phosphorylation of H2AX histone at serine 139. *J Biol Chem* **275**, 9390-5 (2000).

151. Gellert, M. V(D)J recombination: RAG proteins, repair factors, and regulation. *Annu Rev Biochem* **71**, 101-32 (2002).

152. Bassing, C.H. et al. Increased ionizing radiation sensitivity and genomic instability in the absence of histone H2AX. *Proc Natl Acad Sci U S A* **99**, 8173-8 (2002).

153. Burma, S., Chen, B.P., Murphy, M., Kurimasa, A. & Chen, D.J. ATM phosphorylates histone H2AX in response to DNA double-strand breaks. *J Biol Chem* **276**, 42462-7 (2001).

154. Bakkenist, C.J. & Kastan, M.B. DNA damage activates ATM through intermolecular autophosphorylation and dimer dissociation. *Nature* **421**, 499-506 (2003).

155. Paull, T.T. et al. A critical role for histone H2AX in recruitment of repair factors to nuclear foci after DNA damage. *Curr Biol* **10**, 886-95 (2000).

156. Celeste, A. et al. Genomic instability in mice lacking histone H2AX. *Science* **296**, 922-7 (2002).

157. Kobayashi, J. et al. NBS1 localizes to gamma-H2AX foci through interaction with the FHA/BRCT domain. *Curr Biol* **12**, 1846-51 (2002).

158. Rappold, I., Iwabuchi, K., Date, T. & Chen, J. Tumor suppressor p53 binding protein 1 (53BP1) is involved in DNA damage-signaling pathways. *J Cell Biol* **153**, 613-20 (2001).

159. Strahl, B.D. & Allis, C.D. The language of covalent histone modifications. *Nature* **403**, 41-5 (2000).

160. Davie, J.R. & Spencer, V.A. Control of histone modifications. *J Cell Biochem* **Suppl 32-33**, 141-8 (1999).

161. Hunter, N., Valentin Borner, G., Lichten, M. & Kleckner, N. Gamma-H2AX illuminates meiosis. *Nat Genet* **27**, 236-8 (2001).

162. Sarkaria, J.N. et al. Inhibition of phosphoinositide 3-kinase related kinases by the radiosensitizing agent wortmannin. *Cancer Res* **58**, 4375-82 (1998).

163. Siino, J.S. et al. Photobleaching of GFP-labeled H2AX in chromatin: H2AX has low diffusional mobility in the nucleus. *Biochem Biophys Res Commun* **297**, 1318-23 (2002).

164. Nazarov, I.B. et al. Dephosphorylation of histone gamma-H2AX during repair of DNA double-strand breaks in mammalian cells and its inhibition by calyculin A. *Radiat Res* **160**, 309-17 (2003).

165. Mirkovitch, J., Gasser, S.M. & Laemmli, U.K. Scaffold attachment of DNA loops in metaphase chromosomes. *J Mol Biol* **200**, 101-9 (1988).

166. Tubo, R.A. & Berezney, R. Identification of 100 and 150 S DNA polymerase alpha-primase megacomplexes solubilized from the nuclear matrix of regenerating rat liver. *J Biol Chem* **262**, 5857-65 (1987).

167. Abulafia, R., Ben-Ze'ev, A., Hay, N. & Aloni, Y. Control of late simian virus 40 transcription by the attenuation mechanism and transcriptionally active ternary complexes are associated with the nuclear matrix. *J Mol Biol* **172**, 467-87 (1984).

168. Zeitlin, S., Parent, A., Silverstein, S. & Efstratiadis, A. Pre-mRNA splicing and the nuclear matrix. *Mol Cell Biol* **7**, 111-20 (1987).

169. Covey, L., Choi, Y. & Prives, C. Association of simian virus 40 T antigen with the nuclear matrix of infected and transformed monkey cells. *Mol Cell Biol* **4**, 1384-92 (1984).

170. Jackson, D.A. & Cook, P.R. Visualization of a filamentous nucleoskeleton with a 23 nm axial repeat. *Embo J* **7**, 3667-77 (1988).

171. Fawcett, D.W. On the occurrence of a fibrous lamina on the inner aspect of the nuclear envelope in certain cells of vertebrates. *Am J Anat* **119**, 129-45 (1966).

172. Moir, R.D., Spann, T.P. & Goldman, R.D. The dynamic properties and possible functions of nuclear lamins. *Int Rev Cytol* **162B**, 141-82 (1995).

173. Stuurman, N., Sasse, B. & Fisher, P.A. Intermediate filament protein polymerization: molecular analysis of Drosophila nuclear lamin head-to-tail binding. *J Struct Biol* **117**, 1-15 (1996).

174. Liu, J. et al. Essential roles for Caenorhabditis elegans lamin gene in nuclear organization, cell cycle progression, and spatial organization of nuclear pore complexes. *Mol Biol Cell* **11**, 3937-47 (2000).

175. Moir, R.D., Yoon, M., Khuon, S. & Goldman, R.D. Nuclear lamins A and B1: different pathways of assembly during nuclear envelope formation in living cells. *J Cell Biol* **151**, 1155-68 (2000).

176. Hozak, P., Sasseville, A.M., Raymond, Y. & Cook, P.R. Lamin proteins form an internal nucleoskeleton as well as a peripheral lamina in human cells. *J Cell Sci* **108 (Pt 2)**, 635-44 (1995).

177. Nakayasu, H. & Ueda, K. Preferential association of acidic actin with nuclei and nuclear matrix from mouse leukemia L5178Y cells. *Exp Cell Res* **163**, 327-36 (1986).

178. Fey, E.G. & Penman, S. Nuclear matrix proteins reflect cell type of origin in cultured human cells. *Proc Natl Acad Sci U S A* **85**, 121-5 (1988).

179. Amankwah, K.S. & De Boni, U. Ultrastructural localization of filamentous actin within neuronal interphase nuclei in situ. *Exp Cell Res* **210**, 315-25 (1994).

180. Tan, J.H., Wooley, J.C. & LeStourgeon, W.M. Nuclear matrix-like filaments and fibrogranular complexes form through the rearrangement of specific nuclear ribonucleoproteins. *Mol Biol Cell* **11**, 1547-54 (2000).

181. He, D.C., Martin, T. & Penman, S. Localization of heterogeneous nuclear ribonucleoprotein in the interphase nuclear matrix core filaments and on perichromosomal filaments at mitosis. *Proc Natl Acad Sci U S A* **88**, 7469-73 (1991).

182. He, D., Zeng, C. & Brinkley, B.R. Nuclear matrix proteins as structural and functional components of the mitotic apparatus. *Int Rev Cytol* **162B**, 1-74 (1995).

183. Compton, D.A., Szilak, I. & Cleveland, D.W. Primary structure of NuMA, an intranuclear protein that defines a novel pathway for segregation of proteins at mitosis. *J Cell Biol* **116**, 1395-408 (1992).

184. Gueth-Hallonet, C., Wang, J., Harborth, J., Weber, K. & Osborn, M. Induction of a regular nuclear lattice by overexpression of NuMA. *Exp Cell Res* **243**, 434-52 (1998).

185. Harborth, J., Wang, J., Gueth-Hallonet, C., Weber, K. & Osborn, M. Self assembly of NuMA: multiarm oligomers as structural units of a nuclear lattice. *Embo J* **18**, 1689-700 (1999).

186. Foisner, R., Traub, P. & Wiche, G. Protein kinase A- and protein kinase C-regulated interaction of plectin with lamin B and vimentin. *Proc Natl Acad Sci U S A* **88**, 3812-6 (1991).

187. Apel, E.D., Lewis, R.M., Grady, R.M. & Sanes, J.R. Syne-1, a dystrophin- and Klarsicht-related protein associated with synaptic nuclei at the neuromuscular junction. *J Biol Chem* **275**, 31986-95 (2000).

188. Mislow, J.M., Kim, M.S., Davis, D.B. & McNally, E.M. Myne-1, a spectrin repeat transmembrane protein of the myocyte inner nuclear membrane, interacts with lamin A/C. *J Cell Sci* **115**, 61-70 (2002).

189. Zhang, Q. et al. Nesprins: a novel family of spectrin-repeat-containing proteins that localize to the nuclear membrane in multiple tissues. *J Cell Sci* **114**, 4485-98 (2001).

190. Zhang, Q., Ragnauth, C., Greener, M.J., Shanahan, C.M. & Roberts, R.G. The nesprins are giant actin-binding proteins, orthologous to Drosophila melanogaster muscle protein MSP-300. *Genomics* **80**, 473-81 (2002).

191. Zhen, Y.Y., Libotte, T., Munck, M., Noegel, A.A. & Korenbaum, E. NUANCE, a giant protein connecting the nucleus and actin cytoskeleton. *J Cell Sci* **115**, 3207-22 (2002).

192. Mislow, J.M. et al. Nesprin-1alpha self-associates and binds directly to emerin and lamin A in vitro. *FEBS Lett* **525**, 135-40 (2002).

193. Mattagajasingh, S.N. et al. A nonerythroid isoform of protein 4.1R interacts with the nuclear mitotic apparatus (NuMA) protein. *J Cell Biol* **145**, 29-43 (1999).

194. Cook, P.R. RNA polymerase: structural determinant of the chromatin loop and the chromosome. *Bioessays* **16**, 425-30 (1994).

195. Ingber, D.E., and Jamieson, J. D. (ed.) *Cells as tensegrity structures: architectural regulation of histodifferentition by physical forces transduced over basement membrane*, (1985).

196. McCready, S.J. & Cook, P.R. Lesions induced in DNA by ultraviolet light are repaired at the nuclear cage. *J Cell Sci* **70**, 189-96 (1984).

197. Fakan, S., Leduc, Y., Lamarre, D., Brunet, G. & Poirier, G.G. Immunoelectron microscopical distribution of poly(ADP-ribose)polymerase in the mammalian cell nucleus. *Exp Cell Res* **179**, 517-26 (1988).

198. Smith, H.C., Puvion, E., Buchholtz, L.A. & Berezney, R. Spatial distribution of DNA loop attachment and replicational sites in the nuclear matrix. *J Cell Biol* **99**, 1794-802 (1984).

199. Xu, J., Manning, F.C. & Patierno, S.R. Preferential formation and repair of chromium-induced DNA adducts and DNA--protein crosslinks in nuclear matrix DNA. *Carcinogenesis* **15**, 1443-50 (1994).